Master’ s Thesis of Landscape Architecture

CFD analysis of urban wind condition and pollutant diffusion in terms of urban form types

도시 형태에 따른 도시 바람환경 및 오염 물질 확산 CFD 분석

February 2022

Seoul National University
Graduate School of Environment Studies

Landscape Architecture

Yu Lin Shen

CFD analysis of urban wind condition and pollutant diffusion in terms of urban form types

Prof. Song, Youngkeun

Submitting a master's thesis of Public Administration

October 2021

Seoul National University
Graduate School of Environment Studies

Landscape Architecture

Yu Lin Shen

Confirming the master's thesis written by

Yu Lin Shen

December 2021

Chair _____ (Seal)

Vice Chair _____ (Seal)

Examiner _____ (Seal)

CFD analysis of urban wind condition and pollutant diffusion in terms of urban form types

서울대학교 환경대학원 환경조경학과
Yu Lin Shen

위 논문은 서울대학교 및 환경대학원 환경조경학과 학위논문 관련 규정에 의거하여 심사위원의 지도과정을 충실히 이수하였음을 확인합니다.

2022년 2월

위 원 장 _____ (서울대학교 환경대학원 교수)

부위원장 _____ (서울대학교 환경대학원 교수)

위 원 _____ (서울대학교 환경대학원 교수)

Abstract

CFD analysis of urban wind condition and pollutant diffusion in terms of urban form types

Yu Lin Shen
Dept. of Landscape Architecture
Graduate School of Environmental Studies
Seoul National University

Rapid urbanization increases the construction of buildings in urban areas, reduces wind speed in urban areas and affects atmospheric circulation, resulting in various environmental problems. Greening in cities can affect urban wind environment and pollutant diffusion. The study of microclimates in urban areas is essential. Many studies ignore the effect of greening on the urban microclimate, wind environment and pollutant diffusion, and only focus on the structure and density of buildings °In this dissertation, I used CFD models to simulate the impacts of various urban structures and the presence or absence of greening on urban ventilation. Second, a variety of space types and greening types were used to simulate the effects of horizontal and vertical winds. Third, I simulated

the impacts of multiple greening types on the diffusion of pollutants at urban intersections with different structures. In three independent studies, I focused on exploring relationships between urban greening, building structure and pollutant diffusion.

The study area selected Jegi-dong Community Center in the low-rise residential area and Gangnam-gu Office Center in the high-rise commercial area °For detection and monitoring of the urban wind environment and pollutant diffusion, traditional methods include geospatial analysis, comparisons with monitoring station data, and on-the-spot surveys with measuring instruments. However, these methods have relatively high time and cost requirements and relatively low accuracy in small-scale urban spaces. To overcome these limitations, commercial computational fluid dynamics (CFD) models have become an important tool in the simulation of microclimate effects, such as the wind environment, pollutant dispersion, and urban heat island effects. The main advantage of the CFD model is that it allows reduction of the city model to a state approximating reality. In addition, the combination of building information for urban areas and CFD software allows for rapid simulation with high efficiency, assessing not only the wind flow environment but also the path of pollutant diffusion in the city.

The results show that, A study of the large-scale urban wind environment with and without greening showed that greening can provide the function of a windbreak forest in urban ventilation, reducing wind speed in urban areas, and that an appropriate greening layout can also guide wind direction. In a dense urban structure, little wind reaches the

inner area of the city. Compared with a less dense urban structure, wind can more strongly affect the inner area, and greater changes in wind speed occurred in the inner area.

When the study area is perpendicular to the wind direction, regardless of the urban structure, the average wind speed drops sharply. Meanwhile, regardless of wind direction, the combination of low-density two-row multilayer and high-density two-row multilayer plantings of trees and shrubs, which provided most vegetation among the greening methods tested, caused the largest decreases in wind speed. In the built-up area, the average wind speed showed an increasing trend, while average wind speed decreased slightly in the open area Overall, with no greening as the standard, the use of only shrubs as a greening method led to the smallest increase in pollutant concentration, while the use of trees and shrubs together as a greening method led to the largest increase. When pollutant sources exist within the city, greening will have a negative effect, greatly reducing the rate of pollutant diffusion.

Therefore, this study describes a method for simulating urban microclimates using CFD models and is aimed at enabling real-time application of this method to urban planning, offering greater accuracy than the average of previous methods.

Keywords : Computational fluid dynamics, Microclimate, Pollutant diffusion, Urban-like intersections, Street greening

Student ID : 2019-24202

Contents

List of Tables

List of Figures

Chapter 1. Introduction

1. Background

1.1. Urbanization and the importance of the urban wind environment

Rapid urbanization has increased the construction of buildings in urban areas, and this urban densification has reduced wind speed and affected atmospheric circulation in urban areas, leading to various environmental problems (Kang et al. 2020). Urbanization can affect the urban greening layout, natural landscape and urban microclimate on a large scale (Pan et al. 2017). With increasing urbanization, wind patterns in the city will change due to the density of buildings, causing strong gusts around buildings that can cause severe damage (Blocken et al. 2004). Updrafts, downdrafts, turbulence, and countercurrents caused by obstructions are amplified in local areas, resulting in temporary wind speed acceleration, which may cause stronger wind speeds at the pedestrian level, affecting pedestrians in the city (Kim et al. 2000). Therefore, studying the wind environment and ventilation of urban areas is essential.

1.2. Urban ventilation, pollutant diffusion and computational fluid dynamics application

The rapid progression of urbanization is one of the main problems currently driving urban pollution. Rapid urbanization has led to global warming and the climate crisis, which have negative impacts on the urban environment (Farr et al. 2008). Among numerous environmental

problems facing urban areas, air pollution is a harmful pollution type that can directly affect human health. In March 2014, the World Health Organization (WHO) estimated that about 7 million people had died in 2012 due to air pollution, accounting for one-eighth of total deaths worldwide. This number is more than double the previous estimate and confirms that air pollution is now the largest single environmental health risk worldwide. Reducing air pollution can save millions of lives (WHO 2014).

Most people living in urban areas are exposed to poor air quality (WHO 2016). Urban populations make up 54% of the global population, and that proportion is expected to reach 66% in 2050. To improve ventilation capacity and air quality in urban areas, evaluation and improvement of the methods used for simulation of ventilation and pollutant diffusion in urban areas is essential.

For studying the impact of urban ventilation, pollutant diffusion and densification of building clusters on natural urban ventilation, computational fluid dynamics (CFD) has high accuracy and efficiency with low time cost, and has been employed by many researchers (Hang et al. 2010).

Urban aerodynamics CFD originated from groundbreaking research in the late 1970s and 1980s. Typical CFD studies include assessing the influence of the computational domain size, grid resolution, boundary conditions, and turbulence models on the calculation results (Murakami et al. 1989, Baetke et al. 1990, Cowan et al. 1997).

2. Purpose

In this dissertation, I used CFD models to simulate the impacts of various urban structures and the presence or absence of greening on urban ventilation. Second, a variety of space types and greening types were used to simulate the effects of horizontal and vertical winds. Third, I simulated the impacts of multiple greening types on the diffusion of pollutants at urban intersections with different structures. In three independent studies, I focused on exploring relationships between urban greening, building structure and pollutant diffusion.

In Chapter 2, I compared ventilation efficiency in two study areas with and without greening, and assessed the overall wind speed change rate as well as small-scale variations based on different land types in the city. My aims were to quantify ventilation in the city and to observe its rate of change from the results.

In Chapter 3, I reduced the scale of the simulation, using the combination of space types and greening types to simulate the impacts of vertical and parallel winds with and without buildings, and quantified the results.

In Chapter 4, I used the road, one of the major pollutant emission sources in the city, as the simulation object and simulated the influence of various road structures and greening combinations on the diffusion of pollutants.

3. Consideration of Prior Research

Table 1. Examples of advanced research using computational fluid dynamics models

Author and year	Title	Contents
Kang et al. 2017	Development of a computational fluid dynamics model with tree drag parameterizations: Application to pedestrian wind comfort in an urban area	This study evaluated the impact of trees on pedestrian wind comfort in urban areas using a wind comfort standard based on Beaufort Wind Rating (BWS) to study the sensory level of human impacts.
Qin et al. 2020	Influence of site and tower types on urban natural ventilation performance in a high-rise, high-density urban environment	This study used the wind speed ratio (WVR) and local mean air age (MAA) to study the urban ventilation performance of streets and towers in a high-rise, high-density urban environment in Hong Kong.
Jurado et al. 2021	On the minimal wind directions required to assess mean annual air pollution concentration based on CFD results	This study evaluated the annual average concentration based on the results of numerical modeling and comparison with annual air quality standards.
Karim et al. 2011	Modelling reacting, localized air pollution using Computational Fluid Dynamics (CFD)	A CFD approach was used to model reactive NO_2 dispersion from vehicle pollutants released on a dual carriageway in Maidstone, UK.
Amorim et al. 2013	CFD modelling of the aerodynamic effect of trees on urban air pollution dispersion	CFD models were used to test air quality simulation methods for different relative wind directions

Di Sabatino et al. 2007	Simulations of pollutant dispersion within idealized urban-type geometries with CFD and integral models	Using the CFD model Fluent and the atmospheric diffusion model ADMS-Urban, the diffusion of point-source and line-source pollutants in the simplest neutral atmospheric boundary layer, and the diffusion of line-source pollutants in various regular building geometries, were studied.
Sanchez et al. 2017	Modelling NOX concentrations through CFD-RANS in an urban hot-spot using high resolution traffic emissions and meteorology from a mesoscale model	This study used a computational fluid dynamics (CFD) model to obtain spatial distribution of the average concentration in a busy urban area of Madrid (Spain) over several days.
Kwak et al. 2015	Urban air quality simulation in a high-rise building area using a CFD model coupled with mesoscale meteorological and chemistry-transport models	Heterogeneity of building geometry enhanced the vertical transport of pollutants, while heterogeneity of actual mobile emissions along the road limited the emission of pollutants near the surface.
Baik et al. 2007	Modeling reactive pollutant dispersion in an urban street canyon	A CFD model was used to study numerically the diffusion of active pollutants in urban street canyons with a street aspect ratio of 1.

Recent research using CFD to analyze the diffusion of pollutants in cities is outlined in Table 1. In all previous studies, the built-in turbulence and species transmission models of the software were used, while parameters for the specified atmospheric pollutants, such as density and mass fraction, were set according to the study area. Modeling of internal pollutant measurement and other data verification processes have also been studied.

In pioneering studies published this year, increasing attention has been paid to the role of vegetation in the diffusion of urban air pollutants. The first pilot study demonstrated that the use of tree species with higher porosity is beneficial for preventing wind and sand invasion of residential areas. Trees can function as effective windbreaks to block wind and sand invasion. In areas with high levels of particulate pollution, concentration diffusion is affected not only by the porosity of trees but also by the spacing between trees. When the spacing between trees is 10 m, the dust removal rate is 19%–22%. However, trees are not always beneficial. If the spacing between the trees is small, turbulence may occur, increasing dust distribution.

Chapter 2. The Impact of Greening on Urban Ventilation

1. Introduction

With continuing urbanization and an increasing number of high-rise buildings, the likelihood of high-rise buildings guiding fast-moving winds to the level of pedestrians has increased sharply. Therefore, urban designers must understand how the development of urban areas affects wind and thereby impacts pedestrian comfort and safety (Adamek et al. 2017). The design of urban areas should ensure the comfort, health and safety of residents and users (Blocken et al. 2012). In recent years, microclimate simulation studies in urban areas have received increasing attention (Tominaga et al. 2011). Urban ventilation, also known as urban breathability, is defined as the ability of urban areas to dilute pollutants, heat, and moisture through the exchange of air between levels within and above the urban canopy, and early studies have shown that it can play an important role in urban air quality (Panagiotou et al. 2013).

2. Materials and methods

2.1. Study site

Selection of the target site for this study was based on climatic characteristics (thermal environment, wind factors, etc.), land-use characteristics (residential, commercial, industrial, etc.), site characteristics

(urbanized area, adjacent open space, etc.), planned strategic sites, and spatial distribution. Within the Seoul urbanized area, 'urbanized areas with low impermeability ratio (E)' and 'low-rise urbanized areas with high impermeability ratio (G)' are space types in which climate change-responsive urban planning can be readily applied. The 'high-rise building concentration area (H)' includes two of the target sites selected for simulation-focused analysis.

The average and standard deviation (SD) of evaluation results for the thermal environment and wind functions were calculated using thermal environment and wind function analysis results for each urban space type and, assuming that the thermal environment and wind function layers for each type satisfy the normality assumption, with levels of Good (G), Normal (N), and Bad (B) at an interval of 1 SD. For example, Figure 1 shows the evaluation results of the thermal environment based on the wind function. When SD $\leq$ 1, it is Normal (N), and the evaluation value of thermal environment and wind function is SD $<$ 1 or SD. In the case of SD $>$ -1, it was judged that there was a difference from the average and classified as Good (G) or Bad (B). The target sites selected for this study are the Jegi-dong Community Center area, classified as hot and windy in the climate environment rating classification, and Gangnam-gu Office Center, classified as an area of hot wind concern.

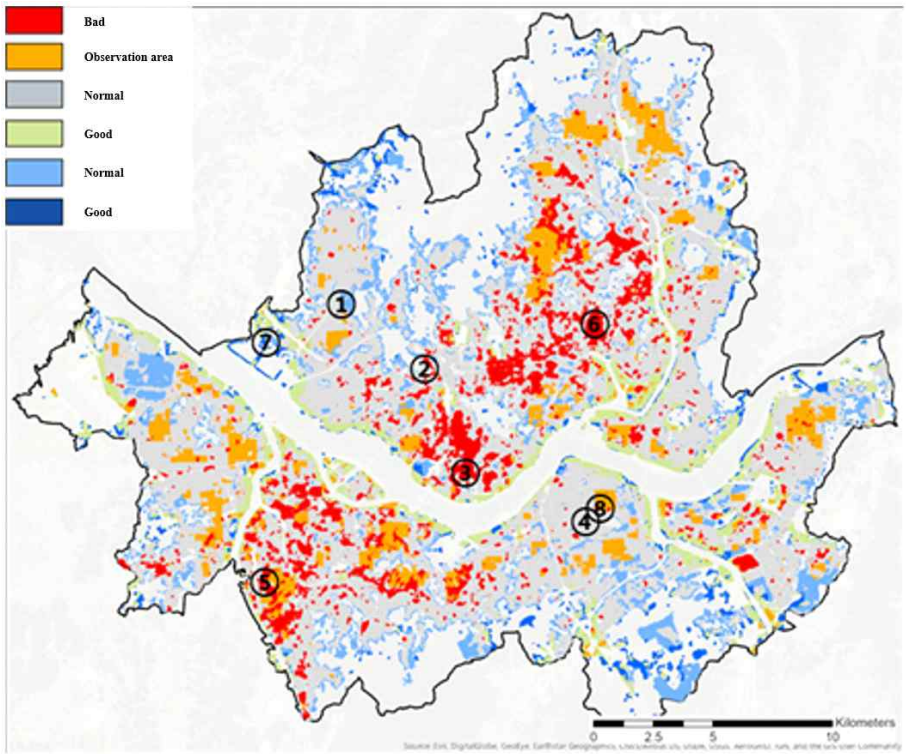

Figure 1. Climatic environment classification results

[G3-(2)] Jegi-dong Community Center

The target site is located in Jegi-dong, Dongdaemun-gu, Seoul, and a fixed fine dust sensor was installed at the Jegi-dong Community Center. Both the thermal environment rating and the wind environment rating of the site were found to be 'bad'.

Low-rise commercial complexes and residential complexes are densely distributed around the site, and the amount of green environment, such as street trees and parks, is insufficient.

The climatic environment of this area can be improved, in all likelihood, through planting of trees on the periphery of a relatively wide

road based on planning techniques and replacement of existing covering with permeable pavement in some areas.

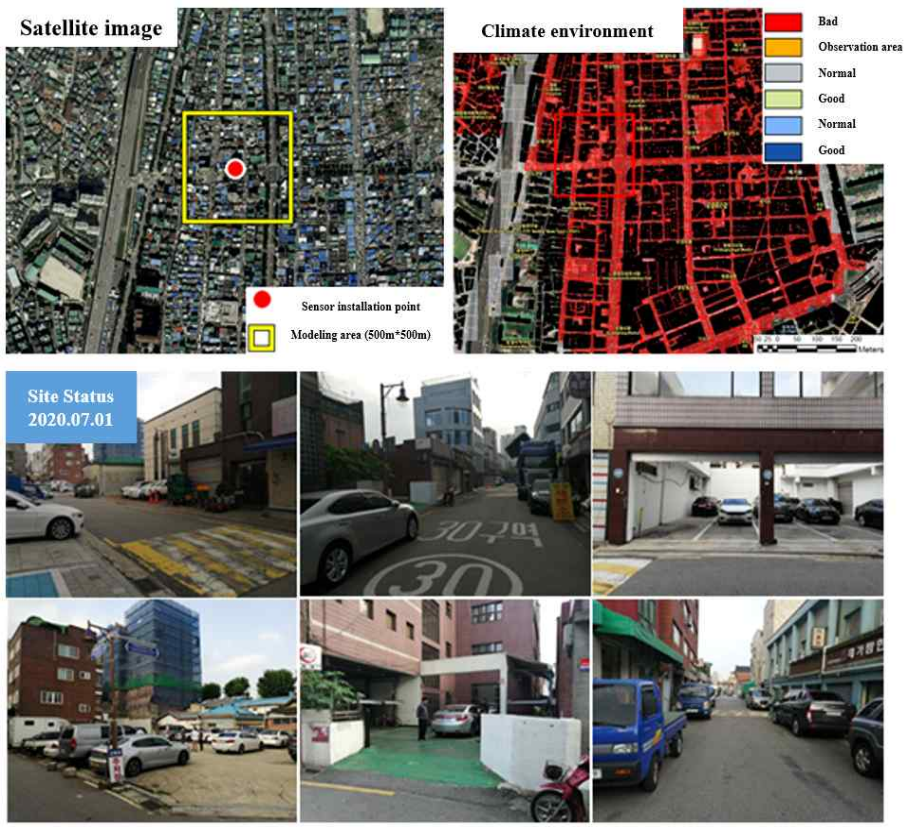

Figure 2. Jegi-dong Community Center

[H3] Gangnam-gu Office Center

As part of the wind road simulation, analysis was conducted to assess the movement of fine dust and pollutants and their transport direction. The analysis sites selected based on the road wind scenario were [H3] Gangnam-gu Office Center and [G3-(2)] Jegi-dong Community Center. Of these sites, [H3] Gangnam-gu Office Center is representative of a high-rise residential area, and [G3-(2)] Jegi-dong Community Center is

representative of a low-rise residential area. [H3] Gangnam-gu Office Center and [G3-(2)] Jegi-dong Community Center were both evaluated using 500 m × 500 m areas.

The location of the study site was evaluated and classified as "Bad" in the climate environment grading of Gangnam-gu, Seoul. Gangnam-gu Office Center adjacent to the boulevard (Hakdong-ro) was selected as the sensor installation area for monitoring. High-rise apartments are clustered around the site, with trees and shrubs planted at the borders of the apartment complex and a children's playground within the apartment complex. Two small parks are located near the site.

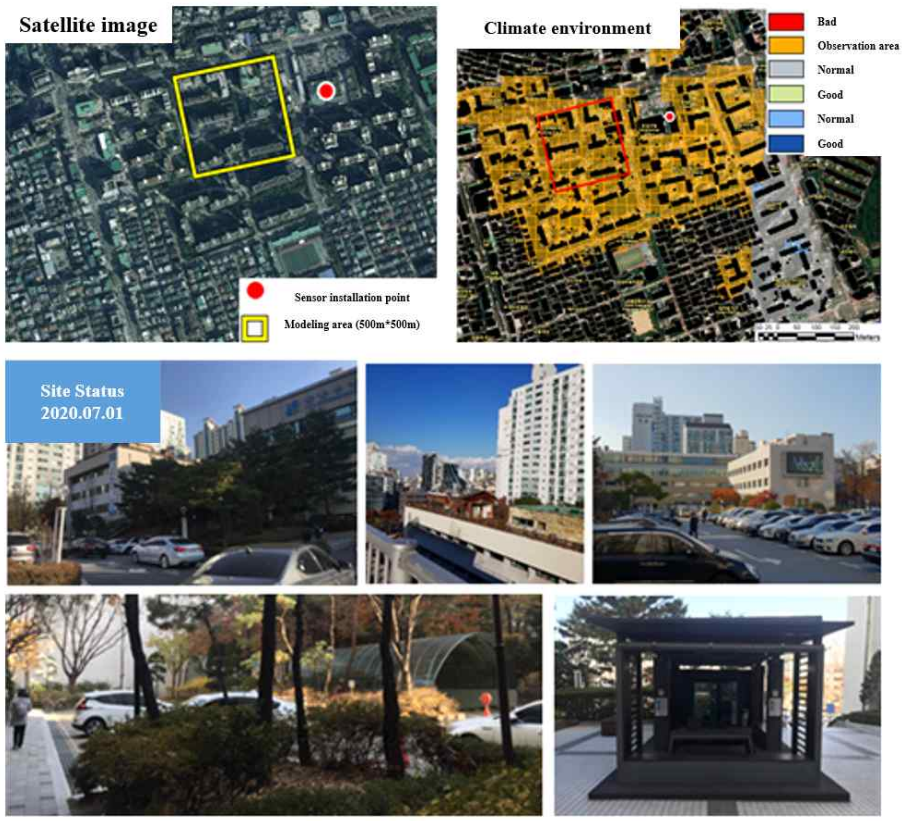

Figure 3. Gangnam-gu Office Center

2.2. Vegetation scenario

The vegetation scenario shown in Figure 4 was based on the size and height of trees and shrubs present in the study area. The tree height is 10 m, the height of the canopy is 7 m, the height of the trunk is 3 m, and the width of the canopy is 7 m. The width and height of the shrub model are both set to 1 m, and the length is set to 3 m.

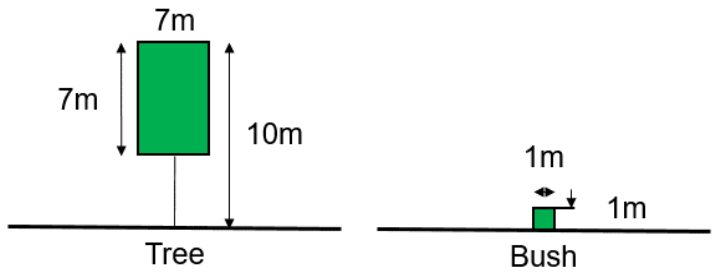

Figure 4. Models of trees and shrubs at the study site

2.3. Obtaining and processing meteorological data

Many weather stations are maintained by the Meteorological Bureau to collect data in Seoul and, therefore, weather data, such as wind direction and wind speed at the target site, is highly accurate. Figure 5 shows wind direction and wind speed statistics for Seoul from January 2019 to February 2020 in the form of a wind direction distribution map. It shows a total of 16 wind directions. Each colored line in the figure represents the wind direction and wind speed during one month of winter. According to the wind direction distribution map, the main wind directions in Seoul in winter are westerly and northwesterly. Although some southerly and easterly winds occur, they are rare. Strong winds occur more frequently in the westerly and northwesterly directions. In winter, the monthly average wind speed increases to 8 m/s, and occasionally reaches 10 m/s. Therefore, in this study, the four directions of north, south, east, and west were used for wind simulation in the two study areas.

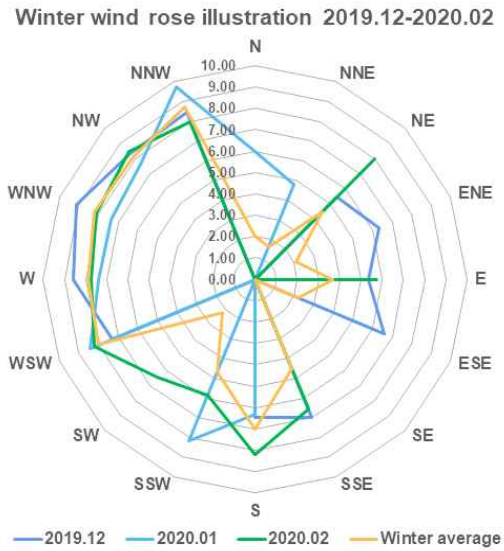

Figure 5. Wind direction distribution in winter (December 2019-February 2020)

2.4. Ansys fluent software simulation process

Prior to simulation, some pre-treatment processes must be undertaken. First, simulating the wind environment or pollutant diffusion in urban areas or local areas of the city requires a reduced model corresponding to exactly the same area. To construct such a model requires building information for the study area, such as the overall height of buildings, the shape of buildings, and height information for each floor. Generally, these data can be found on the official urban space information website of each country. With this building information, a large area can be modeled, and numerous types of modeling software are available for this step. After constructing a model of the research area, geometric processing was conducted in Fluent for preliminary modeling and classification of buildings and vegetation, and then the geometric model

was used to construct a mesh in Fluent. In this step, we set areas as fluid areas or solid areas. To make vegetation a porous medium, as trees are in reality, we make the interior of the vegetation a fluid area, and then set resistance parameters so that it behaves like real vegetation. To simulate pollutant diffusion, we can designate an area as a pollutant emission source. After the mesh is constructed, we enter the simulation stage. In this process, we select a turbulence model. Accuracy and time requirements differ among turbulence models and are often negatively correlated. As accuracy improves, processing efficiency decreases and the calculation time is lengthened. In contrast, reducing accuracy increases efficiency and can greatly shorten the calculation time.

As an effective simulation method for the urban environment, the CFD scheme is widely applied to simulation of the wind environment and diffusion of pollutants in the urban environment. The computational domain size used in this study is X = 1750 m, Y = 1750 m, and Z = 1000 m. To calculate changes in wind speed accurately, mesh refinement was conducted in local areas of the model such as buildings, streets and vegetation.

For all flows, Ansys Fluent solves the conservation equations for mass and momentum. For flows involving heat transfer or compressibility, an additional equation for energy conservation is solved. For flows involving species mixing or reactions, a species conservation equation is solved or, if the non-premixed combustion model is used, conservation equations for the mixture fraction and its variance are solved. Additional transport equations are solved when the flow is turbulent.

Mass Conservation Equation

$$\frac{\sigma\rho}{\sigma t} + \nabla \bullet (\rho\vec{v}) = S_m$$

$$\frac{\sigma\rho}{\sigma t} + \frac{\sigma}{\sigma x}(\rho v_x) + \frac{\sigma}{\sigma \Upsilon}(\rho v_\Upsilon) + \frac{\rho v_\Upsilon}{\Upsilon} = S_m$$

x is the axial coordinate, Υ is the radial coordinate, V_x is the axial speed, and V_Υ is the radial velocity.

Momentum Conservation Equations

$$\frac{\sigma}{\sigma t}(\rho\vec{v}) + \nabla \bullet (\rho\vec{v}\vec{v}) = -\nabla p + \nabla \bullet (\bar{\bar{\tau}}) + \rho\vec{g} + \vec{F}$$

$$\bar{\bar{\tau}} = \mu\left[(\nabla\vec{v} + \nabla\vec{v}^T) - \frac{2}{3}\nabla \bullet \vec{v} I\right]$$

ρ is the static pressure, $\bar{\bar{\tau}}$ is the stress tensor (described below), and $\rho\vec{g}$ and $\bar{\bar{F}}$ are the gravitational body force and external body force, respectively.

The K-epsilon (k-ε) turbulence model is the most commonly used model for CFD simulation of mean flow characteristics under turbulent flow conditions. The k-ε model is a two-equation model that provides a general description of turbulence using two transport equations (PDEs). The original impetus for the k-ε model was improvement of the mixing-length model, and it also provides an alternative to algebraically prescribing turbulent length scales in flows of moderate to high complexity.

Realizable Model

$$\frac{\sigma}{\sigma t}(\rho k) + \frac{\sigma}{\sigma x_j}(\rho k u_j) = \frac{\sigma}{\sigma x_j}\left[\left(\mu + \frac{\mu t}{\sigma_k}\right)\frac{\sigma k}{\sigma x_j}\right] + G_k + G_b - \rho\epsilon - Y_M + S_k$$

$$\frac{\sigma}{\sigma t}(\rho k)+\frac{\sigma}{\sigma x_j}(\rho k u_j)=\frac{\sigma}{\sigma x_j}\left[\left(\mu+\frac{\mu t}{\sigma_k}\right)\frac{\sigma k}{\sigma x_j}\right]+\rho C_1 S\epsilon-\rho C_2\frac{\epsilon^2}{k+\sqrt{v\epsilon}}+C_{1\epsilon}\frac{\epsilon}{k}C_{3\epsilon}G_b+S_\epsilon$$

$$C_1=\max\left[0.43,\frac{\eta}{\eta+5}\right],\quad \eta=S\frac{k}{\epsilon},\quad S=\sqrt{2S_{ij}S_{ij}}$$

Ansys Fluent can model the mixing and transport of chemical species through solution of conservation equations describing the convection, diffusion, and reaction sources for each component species. Multiple simultaneous chemical reactions can be modeled, with reactions occurring in the bulk phase (volumetric reactions), on wall or particle surfaces, in the porous region, and in combinations of these locations. Species transport modeling capabilities, both with and without reactions, are described in this chapter.

Species Transport Equations

$$\frac{\sigma}{\sigma t}(\rho Y_i)+\nabla\bullet\left(\rho\vec{v}Y_i\right)=-\nabla\bullet\vec{J_i}+R_i+S_i$$

R_i is the net rate of production of species i through chemical reactions (described later in this section) and S_i is the rate of creation through addition from the dispersed phase plus any user-defined sources. An equation of this form can be solved for $N-1$ species, where N is the total number of fluid-phase chemical species present in the system. As the mass fractions of all species must sum to unity, the Nth mass fraction is determined as one minus the sum of the $N-1$ solved mass fractions. To minimize numerical error, the Nth species should be selected as the species with the largest overall mass fraction, such as N_2 when the oxidizer is air.

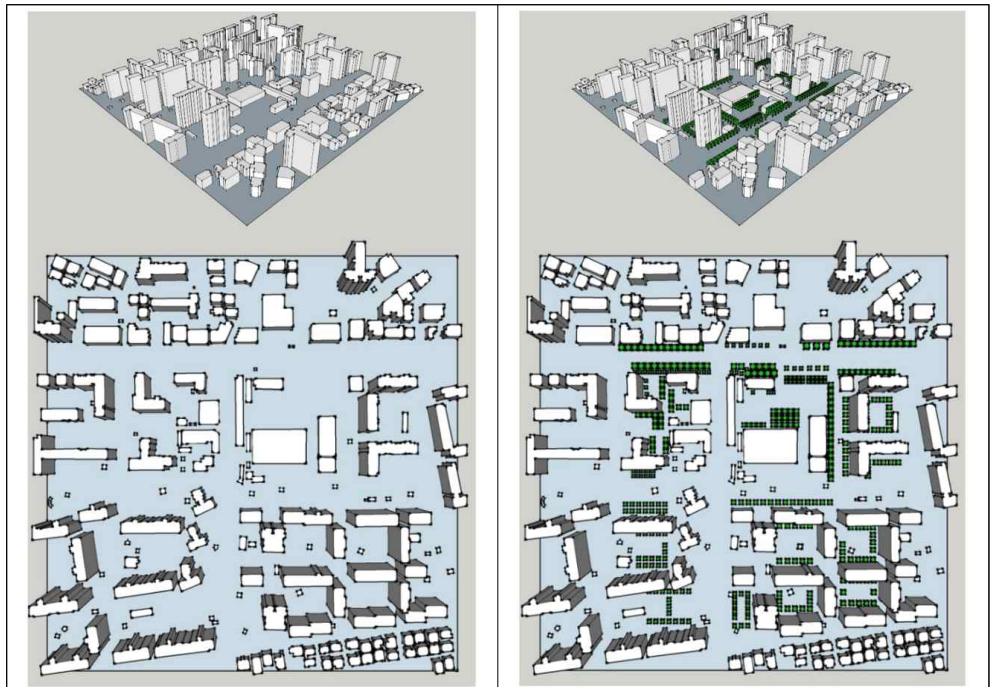

Before greening	After greening

Figure 6. Examples of 3D models around Gangnam-gu Office Center before and after addition of vegetation (left: before greening, right: after greening).

Before greening	After greening

Figure 7. Examples of 3D models around Jegi-dong Community Center before and after addition of vegetation (left: before greening, right: after greening).

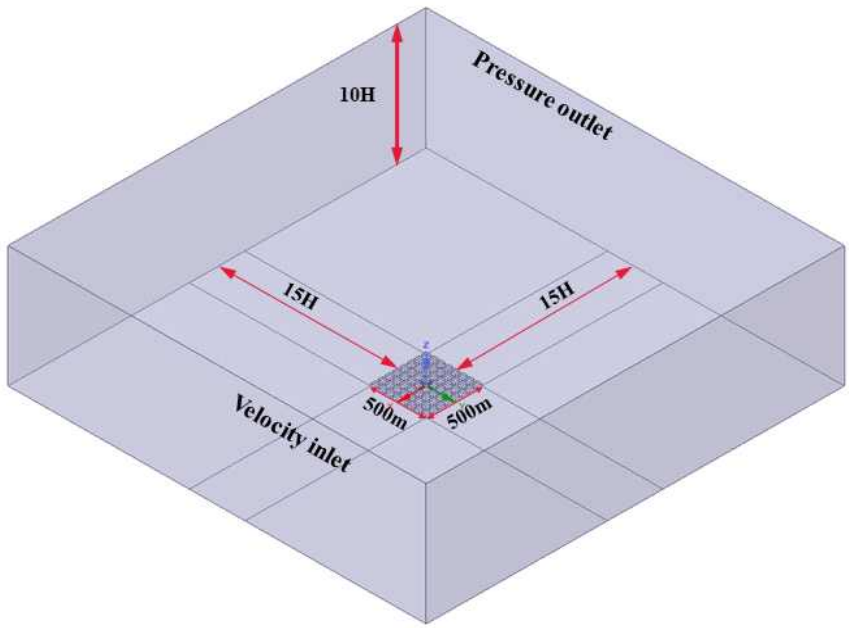

Figure 8. Example calculation area

Data such as building heights and numbers of floors are based on the latest Seoul urban building data for 2019, obtained from the Seoul Urban Spatial Information website. Two scenarios were used in this study, including one case with no trees in the study area, and one case based on a field survey of the actual arrangement of trees in the study area. The models of the study area with and without trees were otherwise identical. The vegetation includes trees and shrubs as greening methods.

3. Results

3.1. Analysis of wind speed changes with greening in Gangnam-gu Office Center

Figures 9 and 10 show average speed contour maps in the four wind directions with and without greening, respectively, in the Gangnam-gu Office Center study area. Overall, average wind speed in the study area always decreases with greening. Trees in the city can function as windbreaks, and their capacity to reduce wind speed within the urban area is high. These figures also show that trees planted in different orientations cause differing overall wind speed changes in the study area. When the wind direction is northerly, the average wind speed decreases by 18.56% with the addition of greenery. When the wind direction is easterly, the average wind speed decreases by 18.10%. When the wind direction is southerly, the average wind speed decreases by 20.29%, and when the wind direction is westerly, a decrease of 21.24% occurs. When the wind direction is perpendicular to the line along which the trees are arranged, relative to parallel wind and planting directions, the trees function better as a windbreak. In the study area, wind from north to south is blocked well by trees along roads and paths, reducing atmospheric circulation within the city. When the wind direction is parallel to the application of greening methods such as trees and shrubs, greenery plays a strong role in guiding the wind.

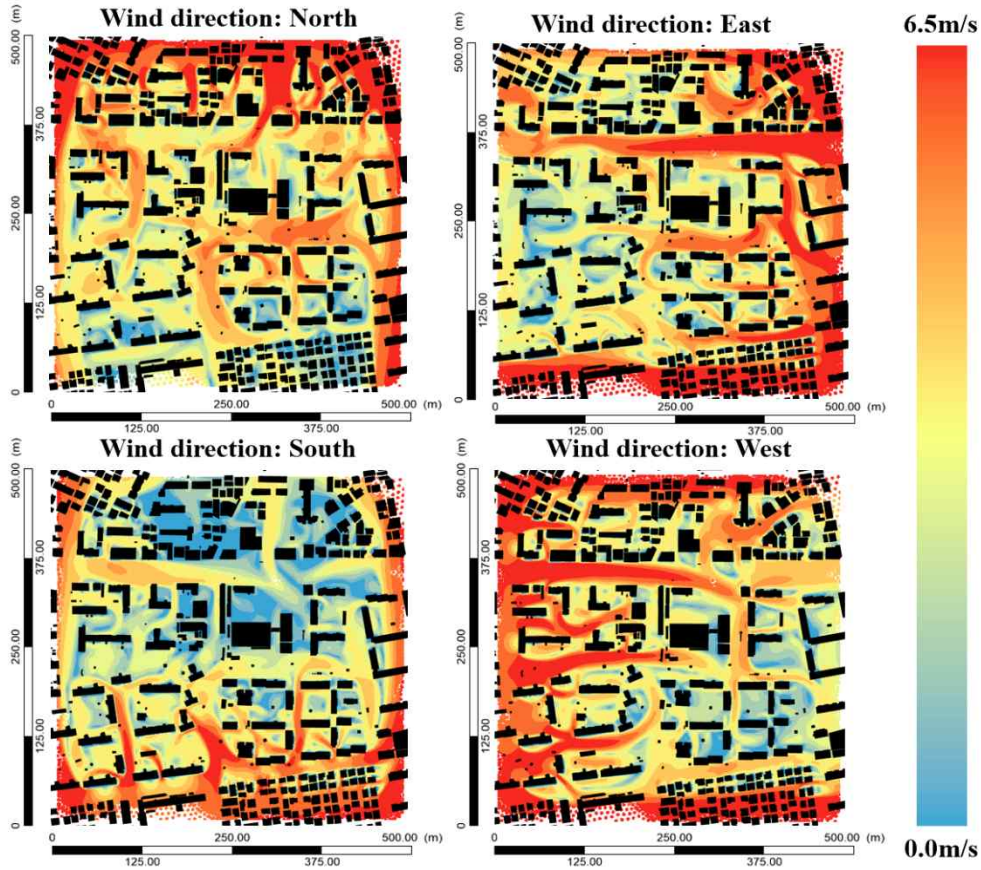

Figure 9. Velocity distribution of Gangnam-gu Office Center (before greening)

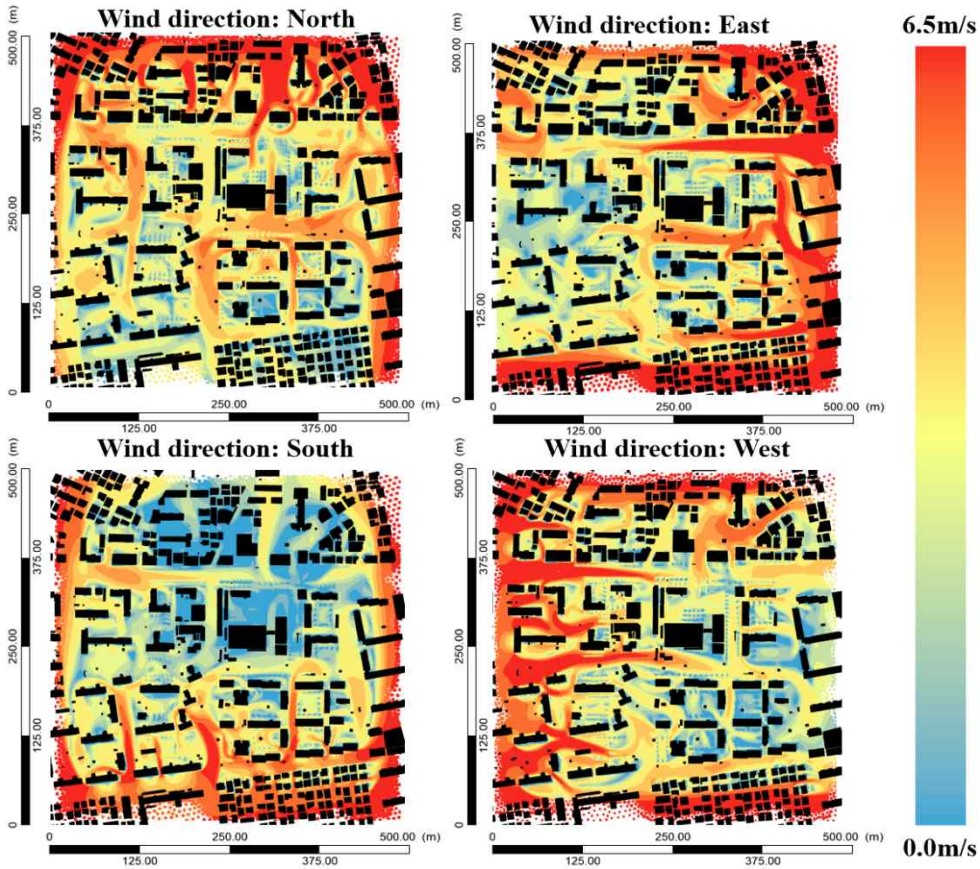

Figure 10. Velocity distribution of Gangnam-gu Office Center (after greening)

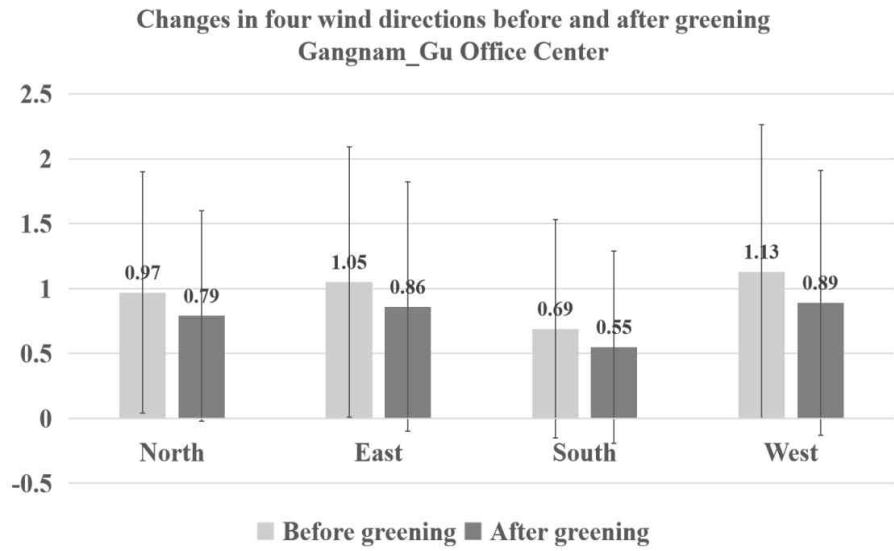

Figure 11. Changes in velocity with greening in four wind directions

Table 2. Rate of change in velocity with greening

Wind direction	Velocity change with vegetation
North	-18.56%
East	-18.10%
South	-20.29%
West	-21.24%

To illustrate the speed changes in four directions with the addition of trees more clearly, I used the difference method to compare speed changes and calculate the maximum speed change in the study area. As shown in Figure 12, areas with large speed changes in the four directions appear near the road and in the open space within high-rise residential buildings in the residential area. In the color key, red represents positive values, indicating a wind speed decrease, while blue represents negative

values, corresponding to increased wind speed. In the east and west wind directions, as shown in Figure 12, the speed of the path area decreases with tree planting, while speeds in residential areas and surrounding open spaces increase. With wind from the north and south wind directions, this figure shows that the road area, residential area and surrounding open space have downward trends in wind speed. Table 3 indicates that the difference in speed with tree planting is largest in the north direction, with a shift from -10.63 m/s to 9.19 m/s, representing a difference of 19.82 m/s. For the east wind direction, the difference in wind speed with tree planting was smallest, from -4.97 m/s to 5.05 m/s, a difference of 10.02 m/s.

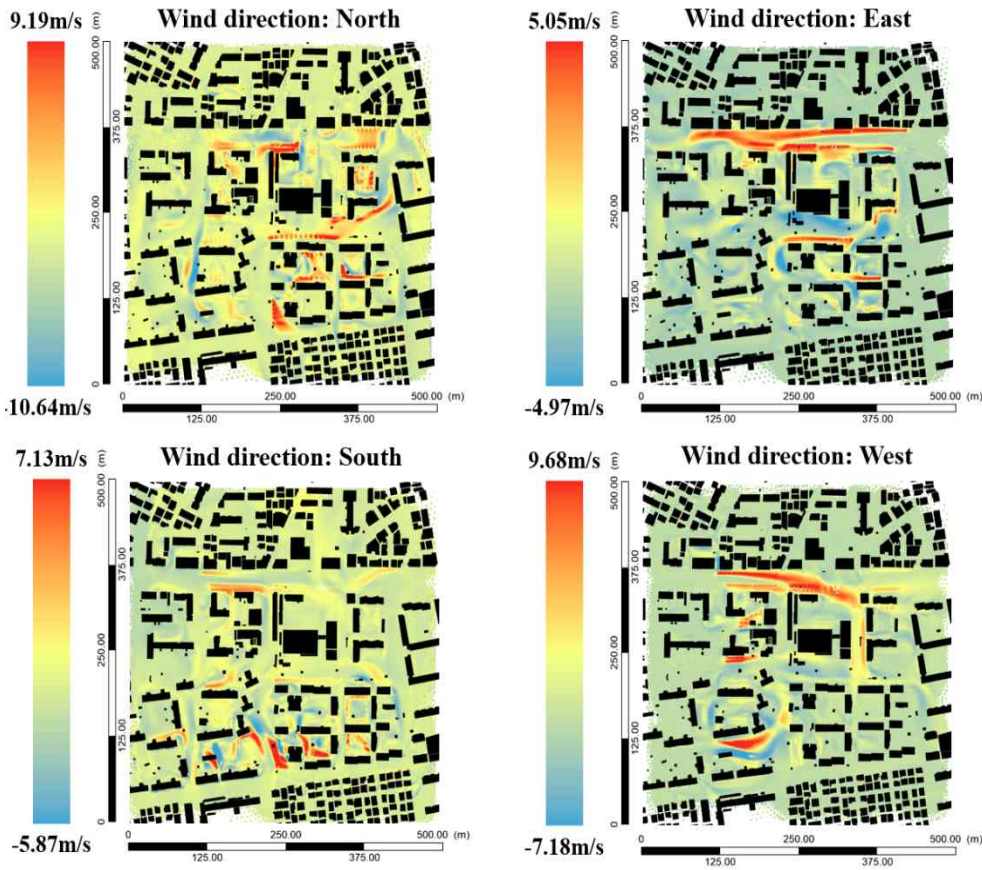

Figure 12. Deviation value of velocity with greening

Table 3. Deviation value of velocity with greening

Wind direction	Wind speed range (m/s)	Deviation value (m/s)
North	-10.63-9.19	19.82
East	-4.97-5.05	10.02
South	-5.87-7.13	13
West	-7.18-9.68	16.86

For estimation of velocity changes in a local area, this study divided land use in the study area into three types: designated open space, road, and path. According to Figure 13 and Table 4, the land type with the largest velocity change is road, which reached -46.63%, and the type with the smallest change is path, at -18.57%. The velocity change is greatest with an east or west wind, when the wind direction is parallel to the arrangement of the trees in the avenue area. This result shows that when wind blows parallel to the arrangement of trees, the trees provide an effective windbreak, reducing wind velocity. According to the results, this reduction can reach 36% to 46%. The flow path is blocked by surrounding high-rise buildings, and the wind does not easily enter the narrow space. Therefore, although the wind speed decreases slightly, the change is relatively small. According to the results of this study, the reduction ranges from 18% to 33%.

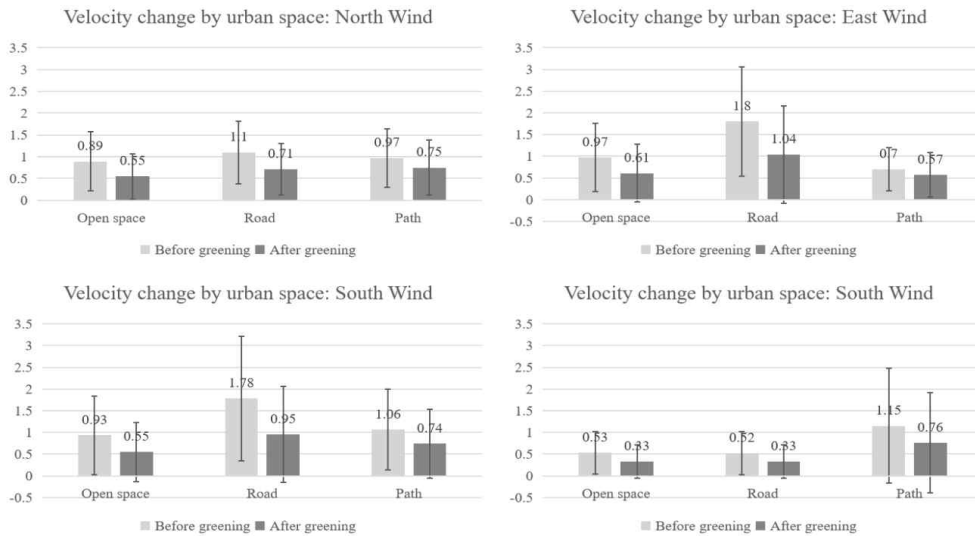

Figure 13. Velocity change by urban space type in Gangnam-gu Office Center

Table 4. Rate of velocity change by urban space type

Wind direction	Open space	Road	Path
North	-38.20%	-35.46%	-22.68%
East	-37.11%	-42.22%	-18.57%
South	-37.74%	-36.54%	-33.91%
West	-40.86%	-46.63%	-30.19%

3.2. Analysis of wind speed changes with greening in Jegi-dong Community Center

Figures 14 and 15 are average velocity distribution diagrams in four wind directions for the Jegi-dong Community Center with and without greening, respectively. Overall, with greening, average speed decreases, as trees in cities can function as windbreaks. The data in Figure 16 and Table 5 show that when the wind direction is northerly, the average wind speed reduction is 25.27%; when the wind direction is easterly, the average wind speed reduction is 33.98%; when the wind direction is southerly, the average wind speed reduction is 28.85%; and when the wind direction is westerly, the average wind speed reduction is 23.86%.

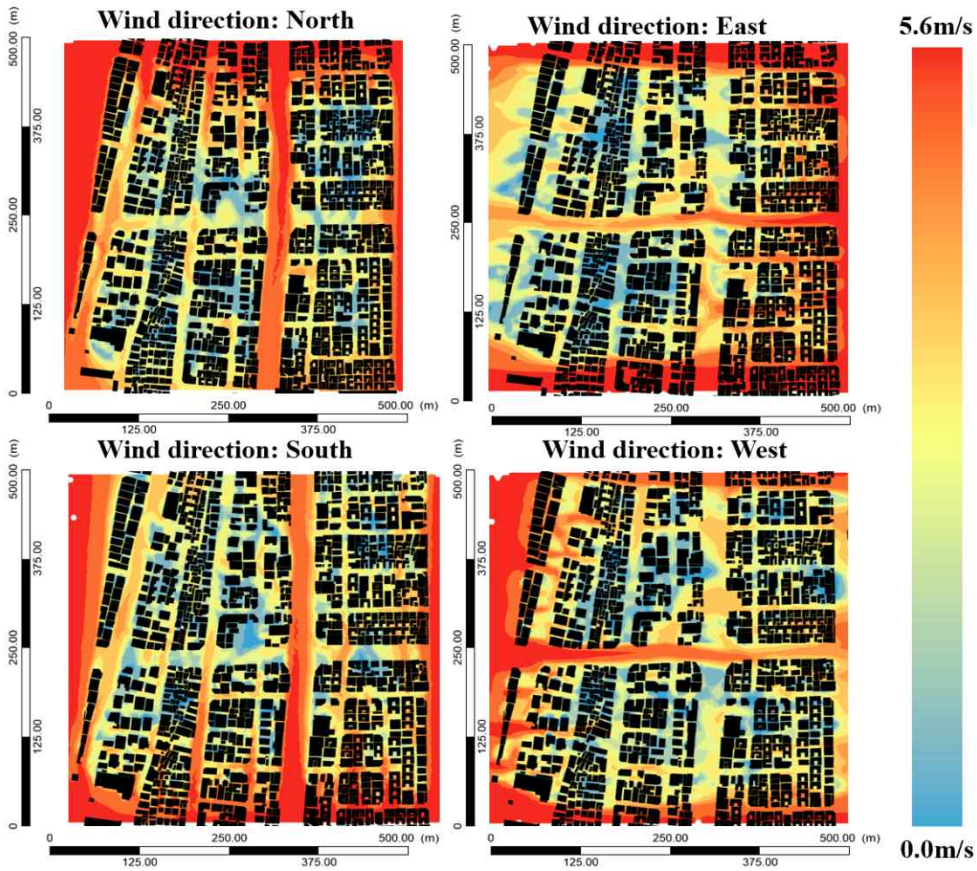

Figure 14. Velocity distribution of Jegi-dong Community Center (before greening)

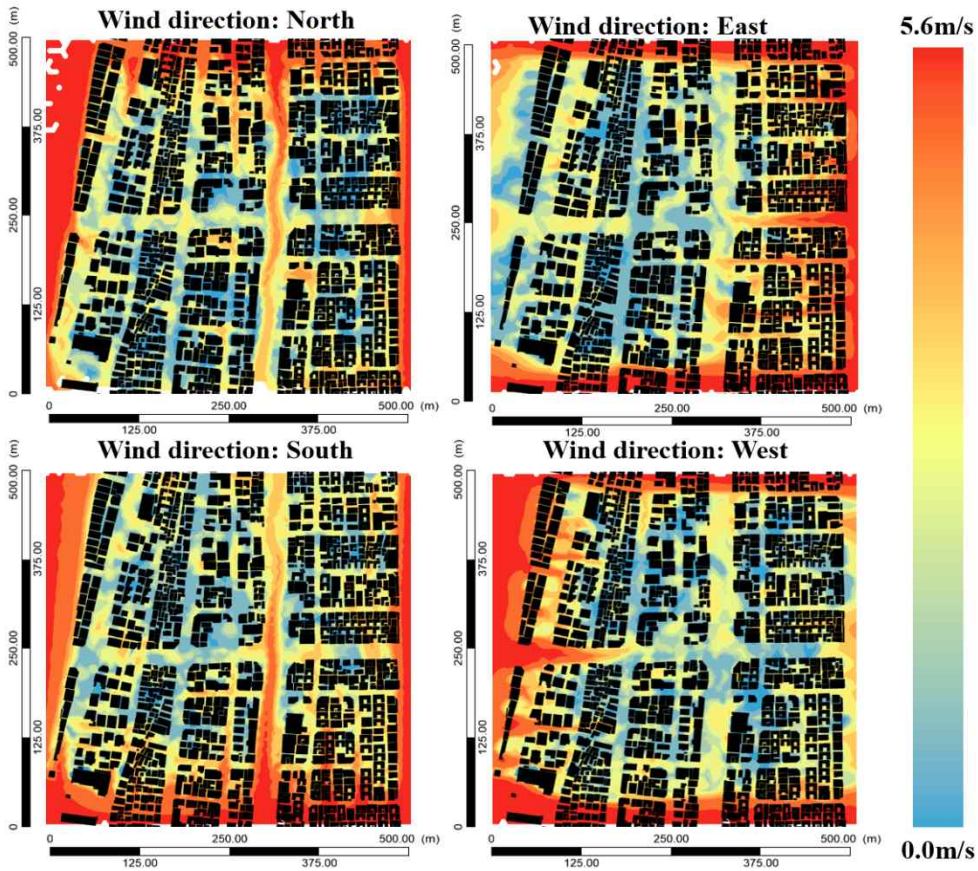

Figure 15. Velocity distribution of Jegi-dong Community Center (after greening)

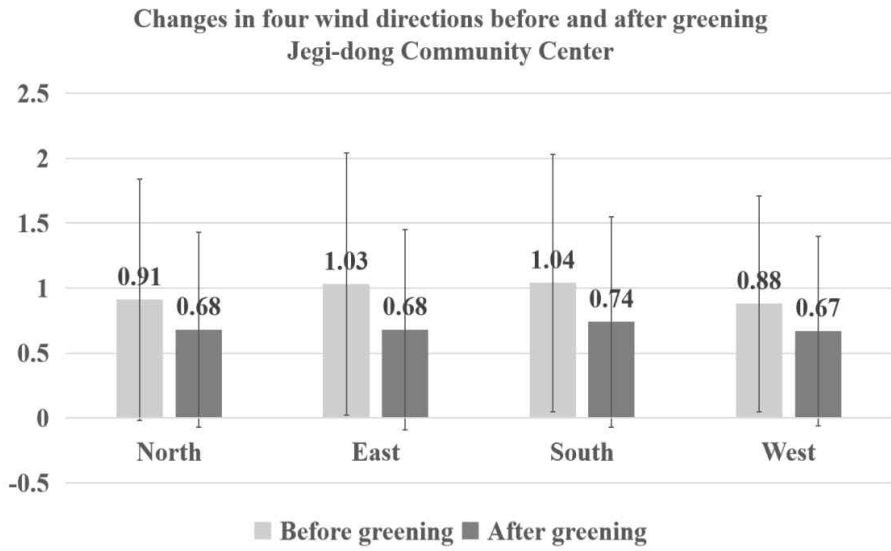

Figure 16. Changes in velocity with greening in four wind directions

Table 5. Rate of change in velocity with greening

Wind direction	Velocity change with vegetation
North	-25.27%
East	-33.98%
South	-28.85%
West	-23.86%

The difference method was used for analysis of wind speed changes in the study area; for this calculation, the wind speed difference under the same wind conditions with and without greenery is determined and areas where wind speed changes are relatively large in the study area are marked. As shown in Figure 17, areas with large speed changes in all four directions are located near the road. The legend indicates that red color represents areas where wind speed decreases, and blue color

represents areas where wind speed increases. The urban structure of this area is a dense low-rise residential area and, therefore, the wind velocity inside the study area shows little change and is relatively stable. The maximum speed change in this area occurs with southerly wind, with a change from -12.01 m/s to 10.63 m/s, representing a difference of 22.64 m/s. The smallest wind speed change is in the east wind direction, from -3.27 m/s to 6.00 m/s, with a difference of 9.27 m/s.

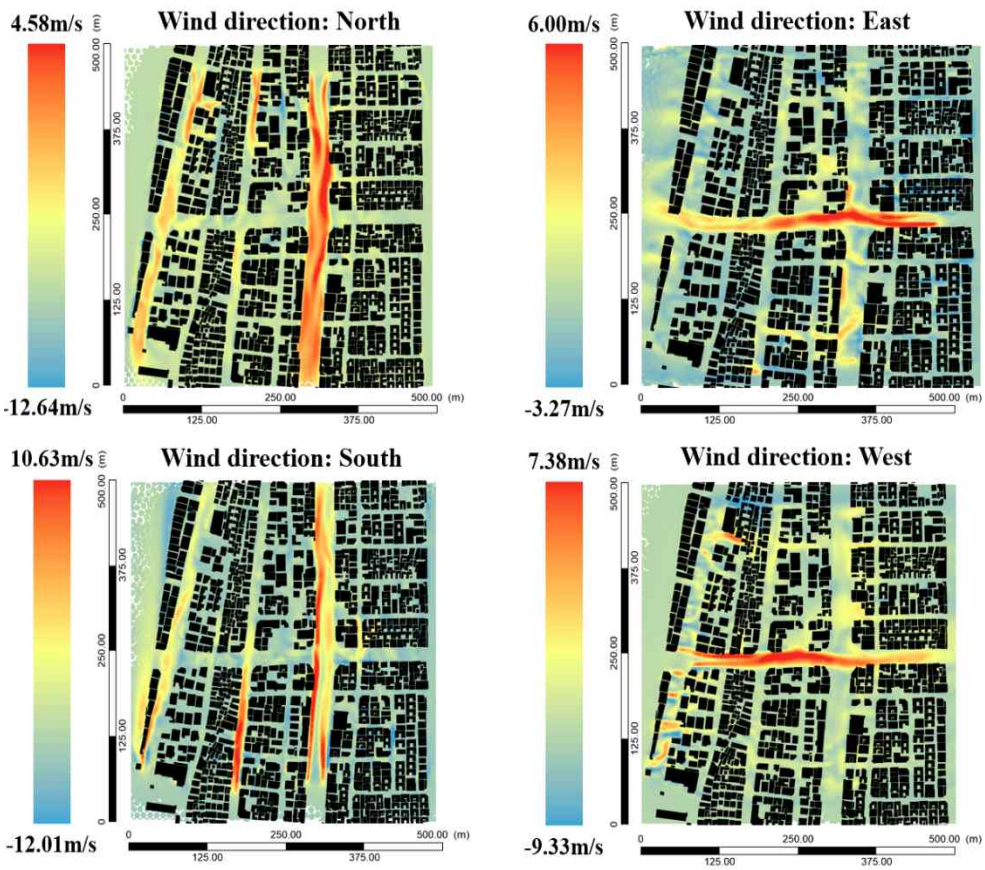

Figure 17. Deviation value of velocity with greening

Table 6. Deviation value of velocity with greening

Wind direction	Wind speed range (m/s)	Deviation value (m/s)
North	-12.64-4.58	17.22
East	-3.27-6.00	9.27
South	-12.01-10.63	22.64
West	-9.33-7.38	16.71

As shown in Figure 18 and Table 7, the land type with the largest velocity change is road, with changes reaching -58.06%, and the type with the smallest change is open space, which reaches only -22.78% variation. The maximum velocity changes occur in the north and east wind directions, which are parallel to the arrangement of trees in the avenue area. This result shows that when the wind direction is parallel to the arrangement of the trees, trees can function effectively as a windbreak and reduce wind velocity. According to the results, this reduction can reach 44%-58%. This area is densely covered with low-rise buildings and its open space is blocked by surrounding high-rise buildings. Wind cannot easily enter the narrow road. Therefore, although the velocity decreases slightly, the change is relatively small. According to the results, this decrease can reach 22%-30%.

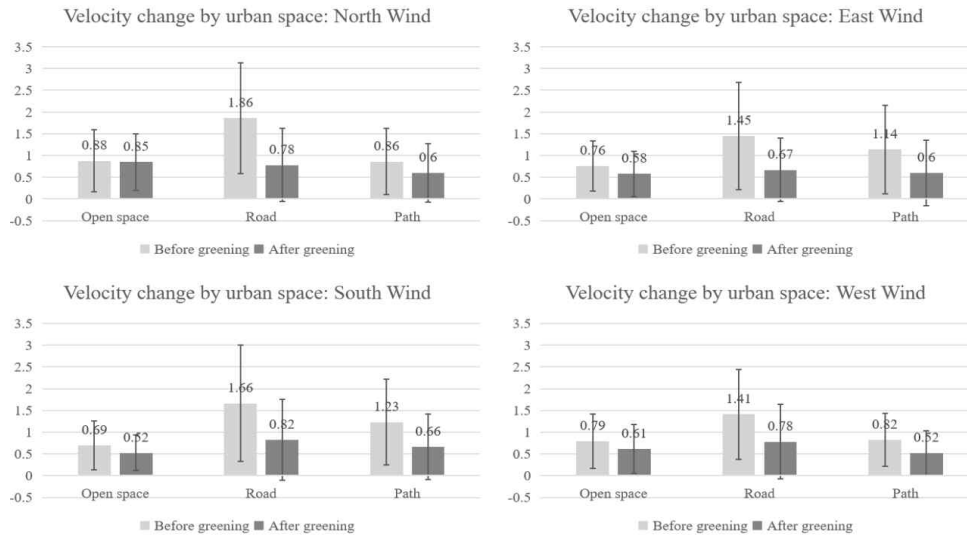

Figure 18. Velocity change by urban space type in Jegi-dong Community Center

Table 7. Rate of velocity change by urban space type

Wind direction	Open space	Road	Path
North	-30.23%	-58.06%	-30.23%
East	-23.68%	-53.79%	-47.37
South	-24.64%	-50.60%	-46.34%
West	-22.78%	-44.68%	-36.59%

4. Discussion

In Chapter 2, we simulated the impact of the presence or absence of greenery in large-scale urban areas on the overall average wind speed in the city, developed a method for distinguishing space types, and compared the average wind speed changes among space types. According to Tables 2 and 5, compared with the case without greening, the overall average wind speed is reduced in both study areas after greening. According to Figures 12 and 17, areas where the average wind speed varies greatly in Gangnam-gu Office Center are concentrated along the main roads and residential areas. Most areas show reductions, while some areas show increases in local average wind speed. The areas with large changes of average wind speed in Jegi-dong Community Center are mainly concentrated along main and small roads, while the interior of the residential area is not strongly affected by wind. The difference between the two study areas arises from the differing density of buildings. Gangnam-gu Office Center is a high-rise urban structure within a low density area, allowing wind to reach the interior of the area, while Jegi-dong Community Center is in a dense low-rise urban area. Because the buildings are low and dense, wind cannot readily reach inner areas of the site.

Chapter 3. Urban Ventilation According to Space Type

1. Introduction

Urban ventilation is the process of air exchange between the outside and inside of a city. High densities of buildings or greenery in various areas of the city can affect urban ventilation efficiency (Panagiotou et al. 2013). Air permeability of the city is directly related to the air flow pattern between buildings and streets, which is driven by interactions between the large air masses approaching the city and urban buildings. A complex air flow pattern may lead to areas of stagnation and wake formation between buildings and along streets (Soulhac et al. 2008). Wind tunnel experiments and numerical simulations have been used to assess flow mechanisms along a street or at two intersecting streets in circular, square, or rectangular city models, and the mechanisms of flow passing through street openings, along the street, and across the street were analyzed (Hang et al. 2009). That study showed that the overall urban form, street configuration, and wind direction could significantly affect flow. Turbulence across the street due to rooves is important for ventilation of the street network (Hang et al. 2009). In the previous study, similar to the simulations described in this chapter, flows around single or paired buildings with an average flow direction perpendicular to the building configuration were studied (Wong et al. 1979).

2. Materials and methods

To simulate the change in wind speed associated with vegetation in the horizontal and vertical directions around various building structures in the study area, we used combinations of shrubs and trees in open and dense areas for modeling.

The module domain is 50 m × 50 m, which contains buildings and plants. The module size was selected with consideration given to the appropriate size for identifying changes in wind speed at the target site and the simulation time of each module. To introduce plantings at the target site, scenarios for planting in a single row, in two rows and in multilayer configurations were set based on the actual trees and shrubs used in the study area. The module domain was divided into open space and high-density built-up space types. As both high-density and open spaces are present among the actual buildings in the target area, the module was divided into dense and open space types.

Simulation and analysis were conducted under the assumption that wind blows in the horizontal (northwesterly) direction and shifts to the vertical direction when blowing parallel to plantings.

In the planting modules, trees were set to 10 m in height, 7 m in width around the trunk, 7 m in trunk height, 3 m in ground cover, and 6 m in spacing between trunks, while shrubs were set to 1 m in height, 1 m in thickness, and 6 m in width for multilayered trees and shrubs. Plant density was analyzed by assessing cases of low density and high density by changing the vegetation porosity setting. The wind pass rate was assumed to be 50% at low density and 0% at high density.

Table 8. Vegetation application model by space type

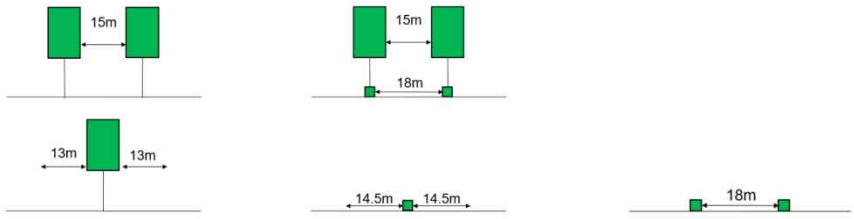

Vegetation type model in open area

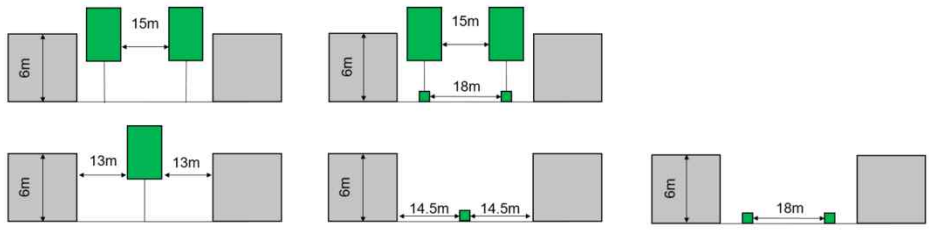

Vegetation type model in a built-up area

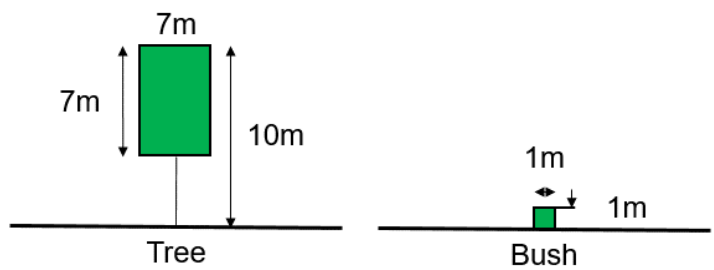

Model for trees and bushes

3. Results

3.1. Horizontal and vertical wind direction simulation in the built-up area

Based on the simulation results obtained with Ansys Fluent, in the urban area, wind that blows horizontally between the building and the planting and parallel to the direction of the building and the planting was confirmed to flow between the planting and the building. However, when the wind blows vertically, the wind speed at the rear of the building decreases due to the building providing a windbreak. In addition, the spacing between buildings can produce an acceleration effect, increasing wind speed (see red box between buildings in the vertical direction). When wind blows vertically, its speed decreases due to the primary blocking effect of the building; vegetation at the rear of the building forms a secondary block, further reducing the wind speed and thereby reducing internal atmospheric circulation in the area. This effect was stronger with two-row multilayer greening than one-row greening. Increasing the spacing between vegetation or the use of low-density vegetation may help to improve atmospheric circulation.

Table 9 shows each space type module, illustrating that a wind path can form when trees are present and the wind blows parallel to the building and planting. This configuration increases wind speed as the wind enters the gap between the building and the planting structure, and the results confirmed that the initial wind input is maintained through to the middle part of the module. Vegetation has a beneficial effect of guiding wind when oriented horizontally (refer to the red box between buildings

and vegetation in the horizontal direction). When wind flows between the building and vegetation on the north side of the module, the wind speed is initially high, and flow is induced between the building and the vegetation. This result demonstrates a positive effect in terms of atmospheric circulation. Design considering both the horizontal and vertical directions of buildings and plantings may be difficult, but appears necessary.

Table 9. Contour maps of wind speed in the parallel and perpendicular directions in the built-up area

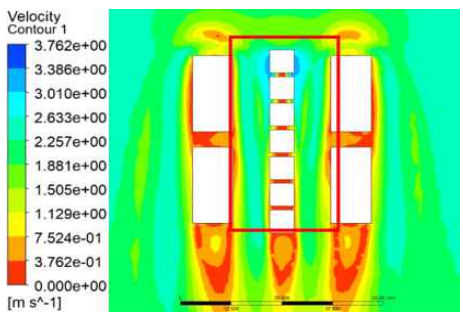	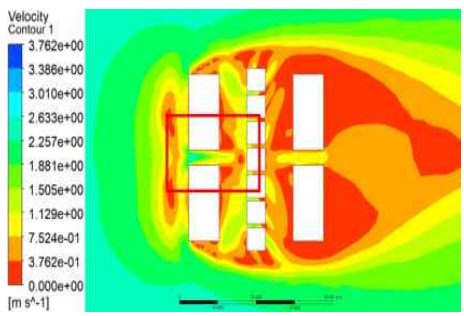
One-row tree (north wind)	One-row tree (west wind)
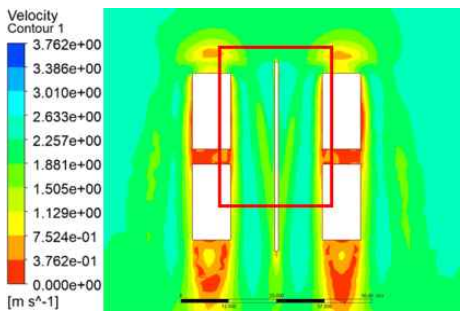	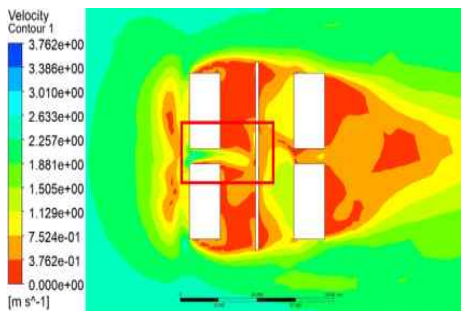
Low-density one-row shrub (north wind)	Low-density one-row shrub (west wind)

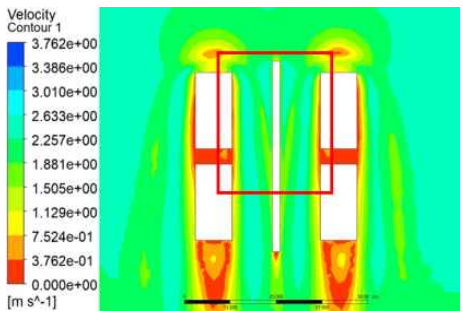	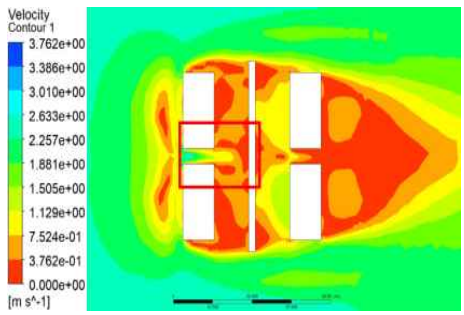
High-density one-row shrub (north wind)	High-density one-row shrub (west wind)
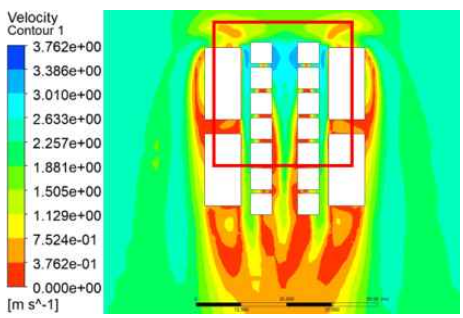	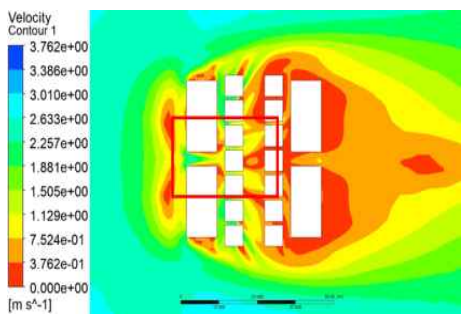
Two-row tree (north wind)	Two-row tree (west wind)
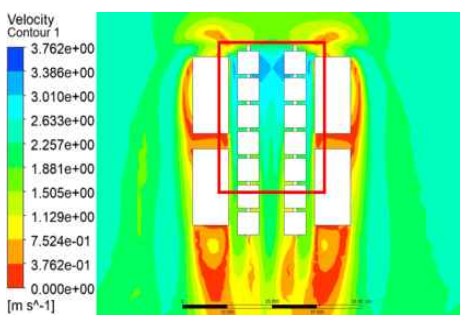	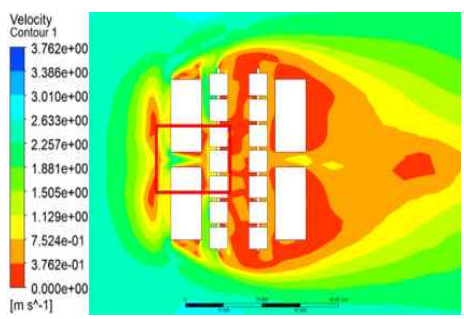
Low-density two-row multilayer (north wind)	Low-density two-row multilayer (west wind)

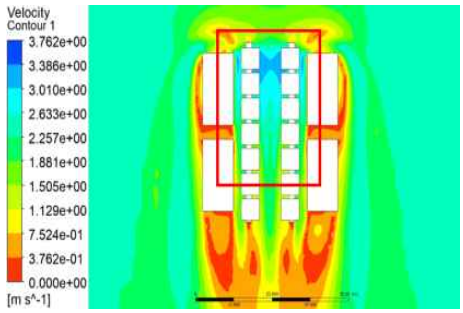	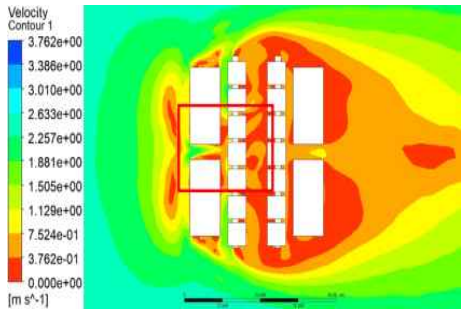
High-density two-row multilayer (north wind)	High-density two-row multilayer (west wind)

Table 10. Example of side view

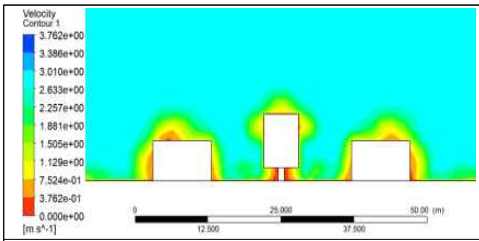	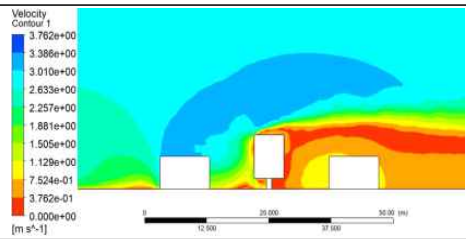
One-row tree (north wind)	One-row tree (west wind)
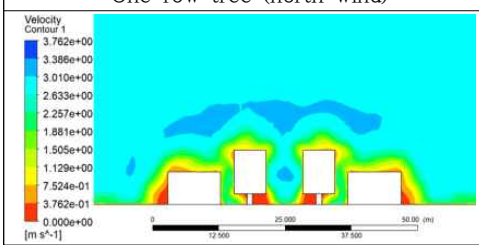	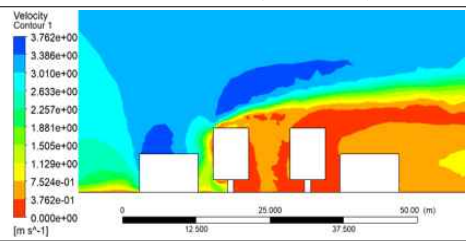
Two-row tree (north wind)	Two-row tree (west wind)
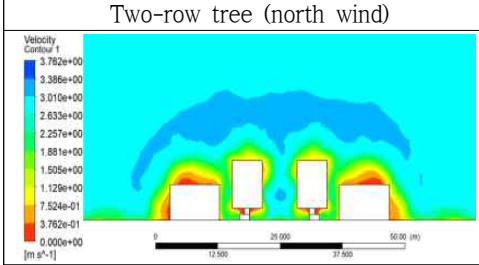	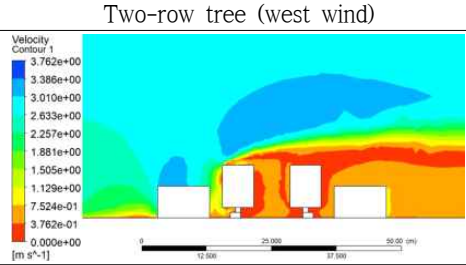
High-density two-row multilayer (north wind)	High-density two-row multilayer (west wind)

Based on the average wind speed for each city type module, greater wind speed changes occur in the vertical direction within the overall planting area than in the horizontal direction. In the urban environment without planting, the average wind speed in the horizontal direction is 1.33 m/s, and the average wind speed in the vertical direction is 1.09 m/s. Without planting, the only structures are those of buildings. The wind speeds differ between the horizontal and vertical directions when the urban area is not planted because the buildings function as windbreaks, providing vertical structure. The highest average wind speed at the horizontal level with a single row of trees is 1.78 m/s, and the lowest average wind speed with a row of low-density shrubs is 1.3 m/s, which is a difference of 0.48 m/s. However, in the vertical direction, the highest average wind speed in the west wind direction with one row of trees is 1.16 m/s, and the lowest average wind speed in the west wind direction with high-density two-row multilayer planting in the built-up area is 0.62 m/s, a difference of 0.52 m/s.

Compared to modules without planting, in the horizontal structure analysis, the average northerly wind speed in the built-up area with one row of trees increased by 33.84%, while it increased by 22.56% in the built-up area with low-density two-row multilayer planting. In contrast, the average wind speed in the westerly direction decreases in the built-up area with low-density one-row shrub planting. When the wind direction and the building are parallel, wind speed generally increases, whereas when the wind direction and the building are perpendicular, average wind speed generally decreases. The average westerly wind

speed in the built-up area with one-row tree planting increased by 6.42%, while it decreased by 43.12%in the built-up area with high-density two-row multilayer planting. Average wind speed increases due to a rapid increase of wind speed in the inflow area driven by wind induction between the trees. However, in the second row of planting, where trees and shrubs were planted in multiple layers, the distance between the planting and the building is narrower, and thus the average wind speed was lower with one row of planting.

In designing for air movement and ventilation in an urban area, simply changing the average amount of planting is insufficient; instead, the spatial distribution of wind speed must be comprehensively considered to achieve the expected effect of planting on wind flow.

Table 11. Average wind speed and rate of change by space type module: north wind standard (comparison with no greening) (unit: m/s)

Space type module	Average wind speed	Rate of change
No greening	1.33	0 (Default)
One-row tree	1.78	+33.84%
Low-density one-row shrub	1.3	-2.26%
High-density one-row shrub	1.4	+5.26%
Two-row tree	1.54	+15.79%
Low-density two-row multilayer	1.63	+22.56%
High-density two-row multilayer	1.56	+17.29%

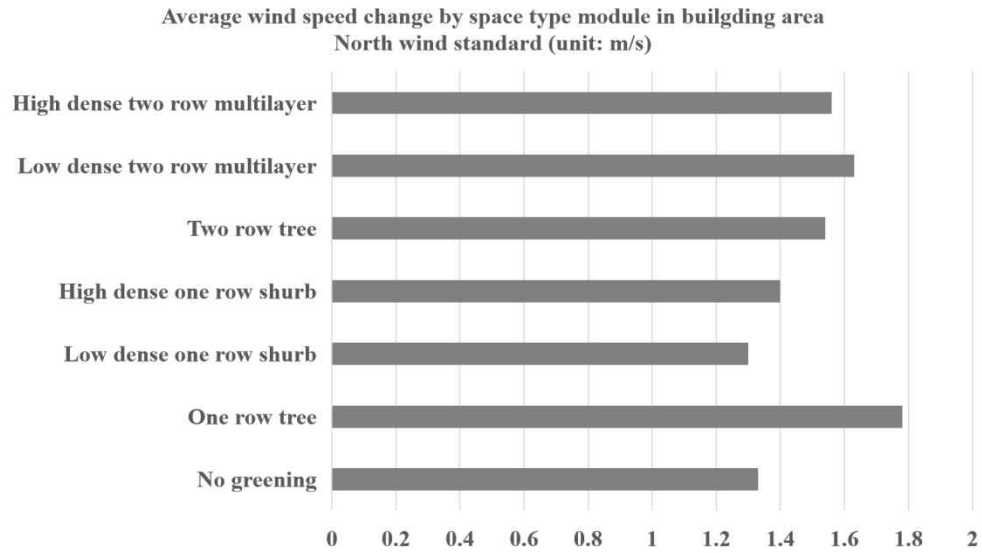

Figure 19. Average wind speed and rate of change in the built-up area according to space type module: north wind standard (unit: m/s)

Table 12. Average wind speed and rate of change for each space type module: west wind standard (comparison with no greening) (unit: m/s)

Space type module	Average wind speed	Rate of change
No greening	1.09	0 (Default)
One-row tree	1.16	+6.42%
Low-density one-row shrub	0.7	-35.78%
High-density one-row shrub	0.8	-26.61%
Two-row tree	1.05	-3.67%
Low-density two-row multilayer	0.63	-42.20%
High-density two-row multilayer	0.62	-43.12%

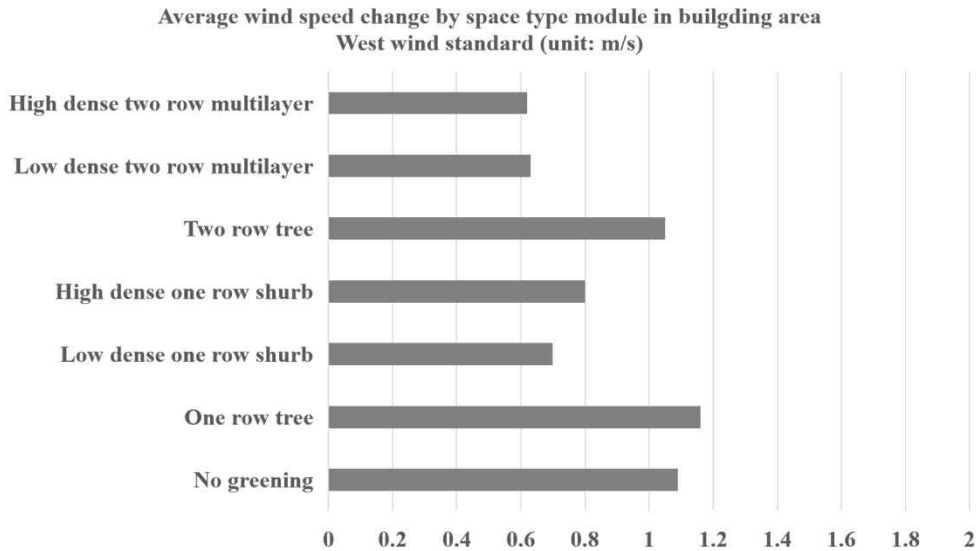

Figure 20. Average wind speed and rate of change in the built-up area according to space type module: west wind standard (unit: m/s)

3.2. Horizontal and vertical wind direction simulation in the open area

Based on the simulation results obtained from Ansys Fluent, when the wind blows horizontally, that is, in a direction parallel to the planting, any difference in spatial distribution within the module configuration is difficult to observe. For the simulation, the wind speed input value was 2.76 m/s, which rose to 3.2 m/s, as indicated with blue colors, between plantings, especially between trees. After setting the wind transmittance of the plantings (trees, shrubs) to 50%, the wind passed through the plantings but did not spread far, especially in the vertical direction. In addition, unlike the urban area, there are no buildings to function as windbreaks; therefore, the change was greater with two rows of planting than with one row.

In the horizontal direction, vegetation played a greater role in inducing wind, although wind speed was not significantly altered, and the extent of the change in wind speed was relatively small. In the vertical direction, plantings can provide a windbreak, affecting the wind speed. The vertical analysis results show that when only trees are planted, the distance between trees is narrow, causing the wind to accelerate between each pair of trees, whereas when trees and shrubs are planted together, the blocking effect on acceleration of the low-level shrubs generates turbulence around the planting. Increased wind speed can be unpleasant for pedestrians. On the other hand, increased wind speed has a positive effect on the diffusion of pollutants.

When applied to an actual site, consideration of both vertical and horizontal impacts of planting is difficult, but planting types can be selected to achieve a suitable shape for wind at the target site.

Table 13. Contour maps of wind speed in the parallel and perpendicular directions in the open area

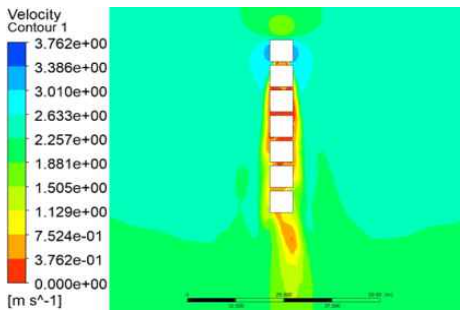	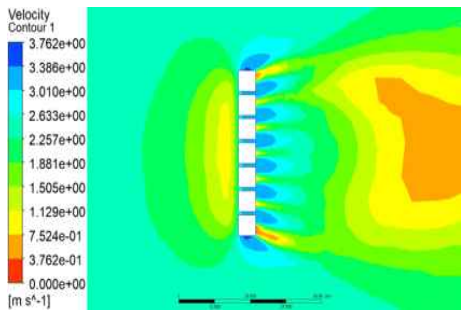
One-row tree (north wind)	One-row tree (west wind)
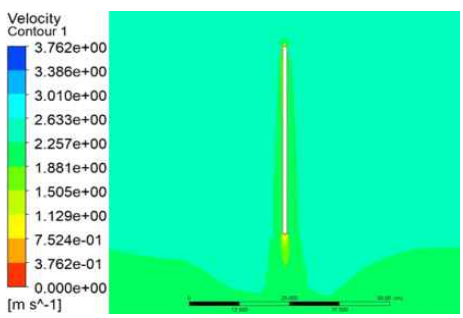	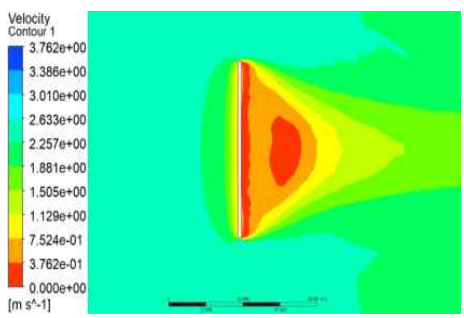
Low-density one-row shrub (north wind)	Low-density one-row shrub (west wind)
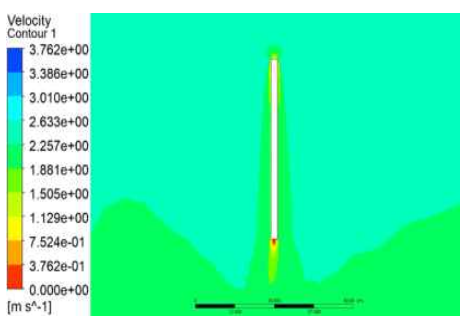	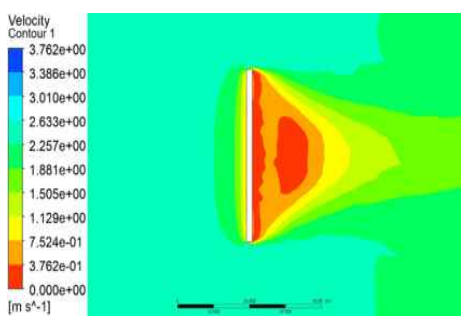
High-density one-row shrub (north wind)	High-density one-row shrub (west wind)

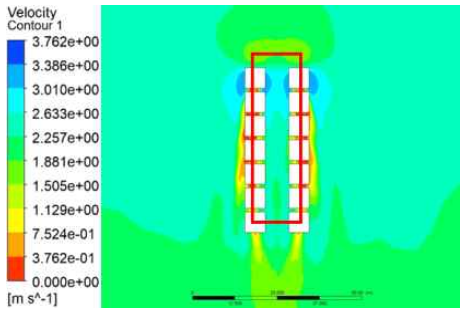

Two-row tree (north wind)

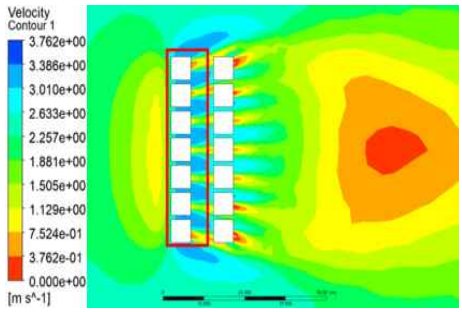

Two-row tree (west wind)

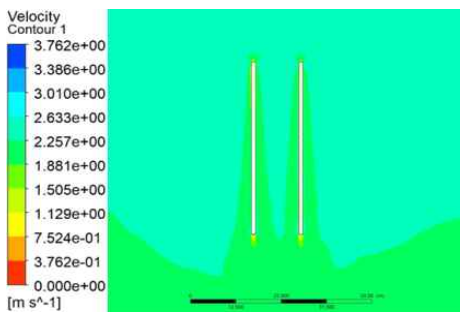

Low-density two-row shrub (north wind)

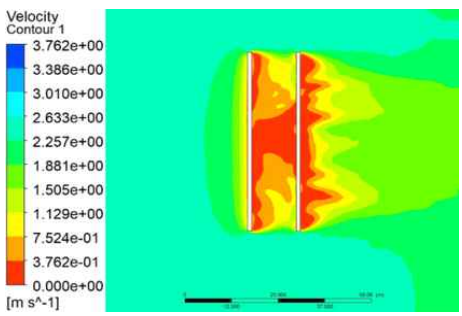

Low-density two-row shrub (west wind)

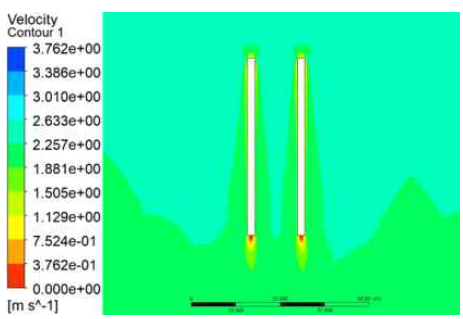

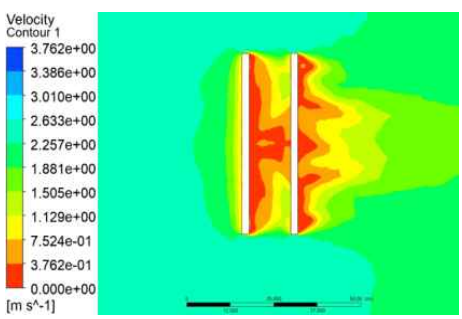

High-density two-row shrub (north wind)	High-density two-row shrub (west wind)
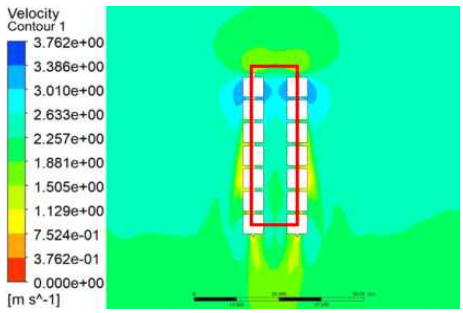	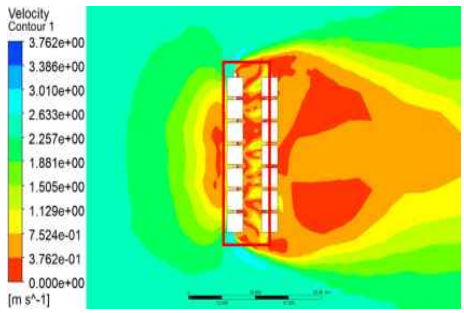
Low-density two-row multilayer (north wind)	Low-density two-row multilayer (west wind)
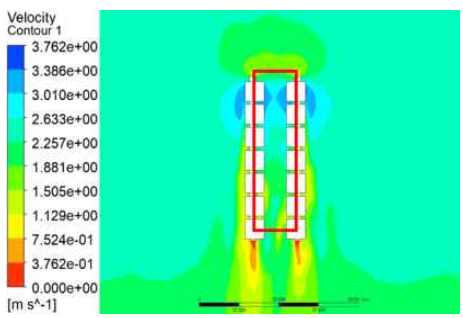	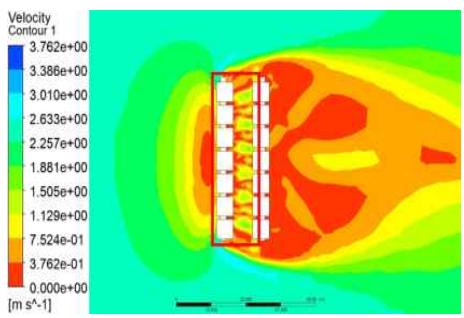
High-density two-row multilayer (north wind)	High-density two-row multilayer (west wind)

Table 14. Example of side view

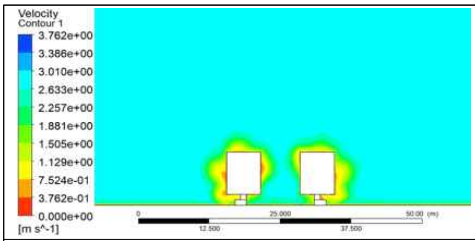	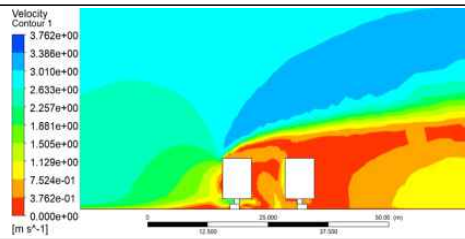
High-density two-row multilayer (north wind)	High-density two-row multilayer (west wind)
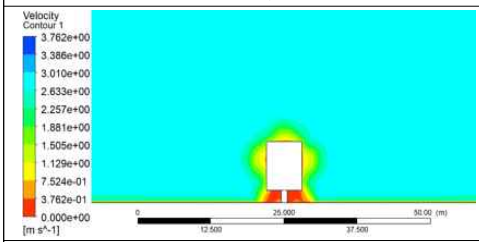	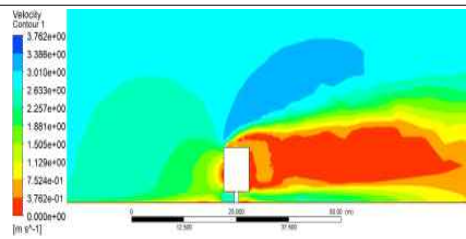
One-row tree (north wind)	One-row tree (west wind)
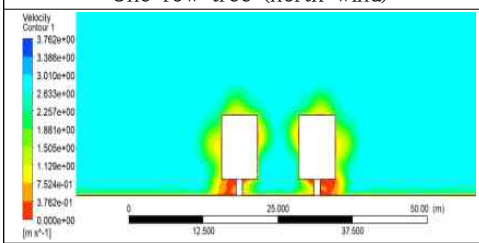	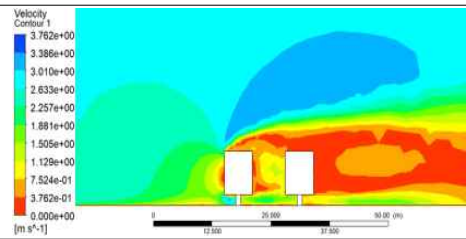
Two-row tree (north wind)	Two-row tree (west wind)

Based on the average wind speed in the open area according to the module, the overall change in wind speed is due to vertical planting structure, not horizontal planting structure. This finding is similar to the flows observed in the built-up area. With a northerly wind, the highest average wind speed in the open area with low-density one-row shrub planting is 1.97 m/s, and the lowest average wind speed in the open area with two-row tree planting is 1.41 m/s, resulting in a difference of 0.42 m/s. However, with a westerly wind, the highest average wind speed in the open area with one row of shrubs is 1.63 m/s, and the lowest average wind speed in the open area with low-density two-row multilayer

planting is 0.66 m/s. Between low-density multilayer and high-density multilayer planting, a structural difference exists between one and two rows of shrubs, but no difference in actual average wind speed was observed.

In terms of proportions, based on the unplanted modules, the average wind speed with two-row tree planting and a westerly wind decreased by 29.5%, while the average wind speed with high-density two-row shrub planting and a westerly wind dropped by 22.5%. With a northerly wind, the average wind speed in the open area with low-density two-row multilayer planting decreased by 68.12%, whereas with a westerly wind, the average wind speed in the open area with high-density two-row shrub planting decreased by 59.9%. In contrast to the built-up area, the average wind speed associated with westerly or northerly winds in the open area decreases with planting, and this decrease is greater with a westerly wind.

If urban design is undertaken based on the current analysis results, the target site would obtain more effective wind protection through the planting of shrubs and trees together, rather than planting only trees. The main effect arises from the planting of trees. Based on the type of urban area, the spatial distribution of wind speed must be considered, rather than simply using an average value for plantings.

Table 15. Average wind speed and rate of change for each space type module: north wind standard (comparison with no greening) (Unit: m/s)

Space type module	Average wind speed	Rate of change
No greening	2	0 (Default)
One-row tree	1.75	-13%
Low-density one-row shrub	1.97	-2%
High-density one-row shrub	1.83	-8%
Two-row tree	1.41	-30%
Low-density two-row shrub	1.89	-6%
High-density two-row shrub	1.55	-23%
Low-density two-row multilayer	1.95	-3%
High-density two-row multilayer	1.91	-5%

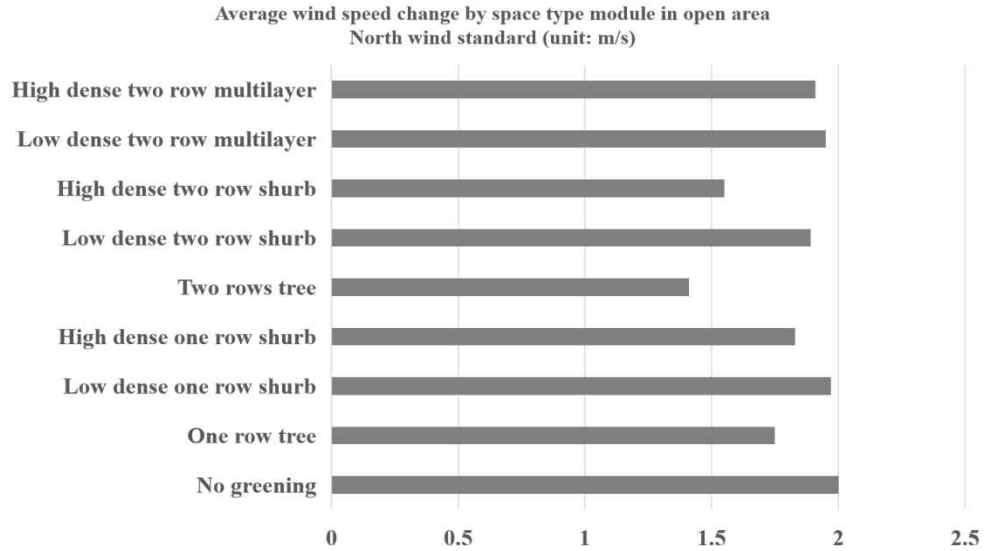

Figure 21. Average wind speed and rate of change in the open area according space type module: north wind standard (unit: m/s)

Table 16. Average wind speed and rate of change for each space type module: west wind standard (comparison with no greening) (unit: m/s)

Space type module	Average wind speed	Rate of change
No greening	2.07	0 (Default)
One-row tree	1.63	-21%
Low-density one-row shrub	1.19	-43%
High-density one-row shrub	1.12	-46%
Two-row tree	1.2	-42%
Low-density two-row shrub	0.92	-56%
High-density two-row shrub	0.83	-60%
Low-density two-row multilayer	0.66	-68%
High-density two-row multilayer	0.66	-68%

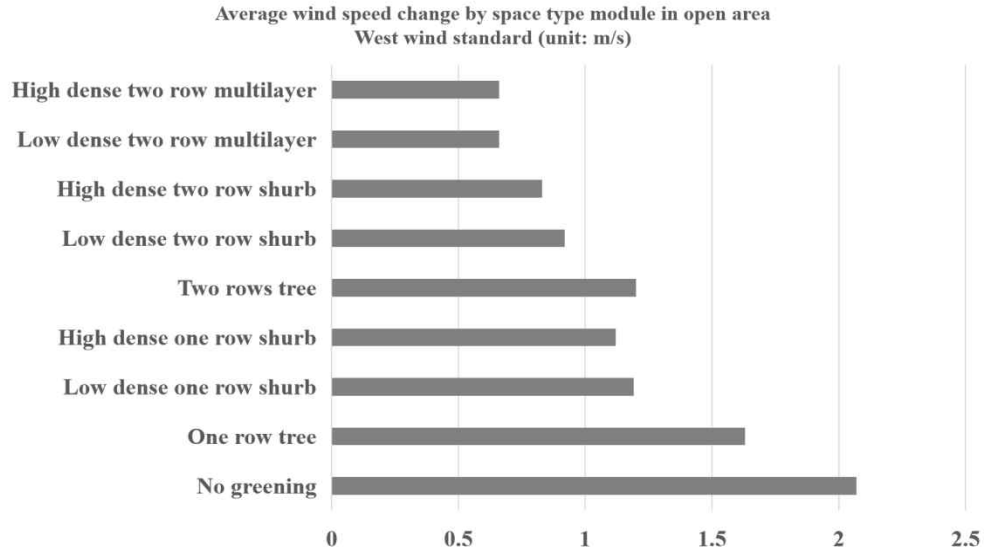

Figure 22. Average wind speed and rate of change in the built-up area according to space type module: west wind standard (unit: m/s)

4. Discussion

In Chapter 3, we simulated a small-scale (50 × 50 m) downwind environment using two common urban structures: an area with buildings and an open area without buildings. The average wind speeds of the two structural areas in directions parallel and perpendicular to the wind direction were studied. Overall, in the built-up area, the average wind speed decreased most sharply in the westerly wind direction (perpendicular wind direction), and the greatest reduction occurs with high-density two-row multilayer planting. The average wind speed decrease reaches 43.12% in the north wind direction (parallel wind direction). The average wind speed shows an increasing trend. The largest increase occurs with low-density two-row multilayer planting, where the average wind speed increase is 22.56%. In the open area, the largest average wind speed decrease with a westerly wind (dominant wind direction) occurs with both low-density two-row multilayer and high-density two-row multilayer planting. The average wind speed decrease reached 68% in the north wind direction (parallel wind direction). The average wind speed decreased the most with two-row tree planting, reaching 30%.

Compared with the built-up area, the average wind speed is generally higher in the open area. This difference arises because no buildings are present to function as a barrier to wind. In both areas, the average wind speed is always lower with a westerly wind than a northerly wind. Thus, in the urban environment, wind direction has a very important influence on wind flows, and the effects of wind reaching the outside of the urban structure will spread to the area inside the urban structure.

Chapter 4. Analysis of Pollutant Diffusion at Urban Road Intersections

1. Introduction

Motor vehicle exhaust is one of the main sources of man-made pollutants in urbanized cities. Due to the surrounding high-rise buildings and narrow streets, wind currents and pollutant transport in the street canyon differs from free flow around the buildings, with complexities due to the geometric shapes of the buildings. Significant research has been conducted into air ventilation, pollutant transport, dilution and removal mechanisms in street canyons. To analyze the movement of pollutants in street canyons, mathematical modeling is usually used due to its low cost and fully controllable parameters (Liu et al. 2005).

Intersections of urban streets are often seriously affected by car exhaust pollution, which causes serious harm to human health (Hlavinka et al. 1988). In such areas, traffic is heavy and people are crowded near roadways. Traffic is often congested due to traffic lights and poor weather. Vehicles often decelerate, stop, start, and accelerate repeatedly. Compared with smooth driving, these changes greatly increase the pollution emission rate. Information about the short-term changes of pollutant concentrations at intersections is limited, but is essential for accurate exposure assessment. In addition, the continuous narrow street canyon shape found at intersections may reduce ventilation and thus the

diffusion of vehicle exhaust, enhancing the accumulation of pollutants in these areas (Guo et al. 2021).

2. Materials and methods

2.1. Study site

The capital of South Korea, Seoul, is also the largest city in South Korea, with heavy traffic and numerous roads. As of December 31, 2020, the number of vehicles in Seoul was approximately 3.15 million. Of national pollutant emissions, emissions in the capital metropolitan area contribute 20% of $PM_{2.5}$, 16% of PM_{10}, 26% of NO_x, 9% of SO_x, 29% of volatile organic compounds, and 19% of NH_3 (Korea Ministry of Environment).

As Seoul is strongly affected by traffic pollutants, the areas of Gangnam-gu Office Center and Jegi-dong Community Center were selected as simulation objects. Figure 1 shows the vegetation layouts of Gangnam-gu Office Center and Jegi-dong Community Center, the two study areas in Seoul. We found that street structures in the two study areas include both cross-shaped intersections and T-shaped intersections. In terms of vegetation, a combination of trees and shrubs are present. In the two study areas, trees are planted closer to the street and shrubs are located closer to the buildings. In the two study areas, more trees are present than shrubs.

Figure 23. Current status of street greening in the study area

2.2. Street structure and greening type

In this study, to assess the impacts of various greening measures on the diffusion of pollutants from urban streets, the greening types shown in Figure 1 were investigated. The height of buildings on both sides of the street was set to 20 m, the distance between buildings (street width) was set to 20 m, the distance between the trees and the buildings was 2 m, the height of the trees was 7 m, the width of the tree crown was 4 m, and the height of the trunk was 3 m. The width and height of the bushes were both set to 1 m, and the length was set to 3 m. In Figure 1, panel a shows the situation without greening, b shows the use of trees as the greening method, c shows a combination of trees and shrubs with shrubs located directly below the trees, d shows only shrubs as the greening method, and e shows the greening method of planting shrubs

near the buildings on both sides of the trees with the distance between the two rows of shrubs set to 2.5 m, to accommodate a sidewalk.

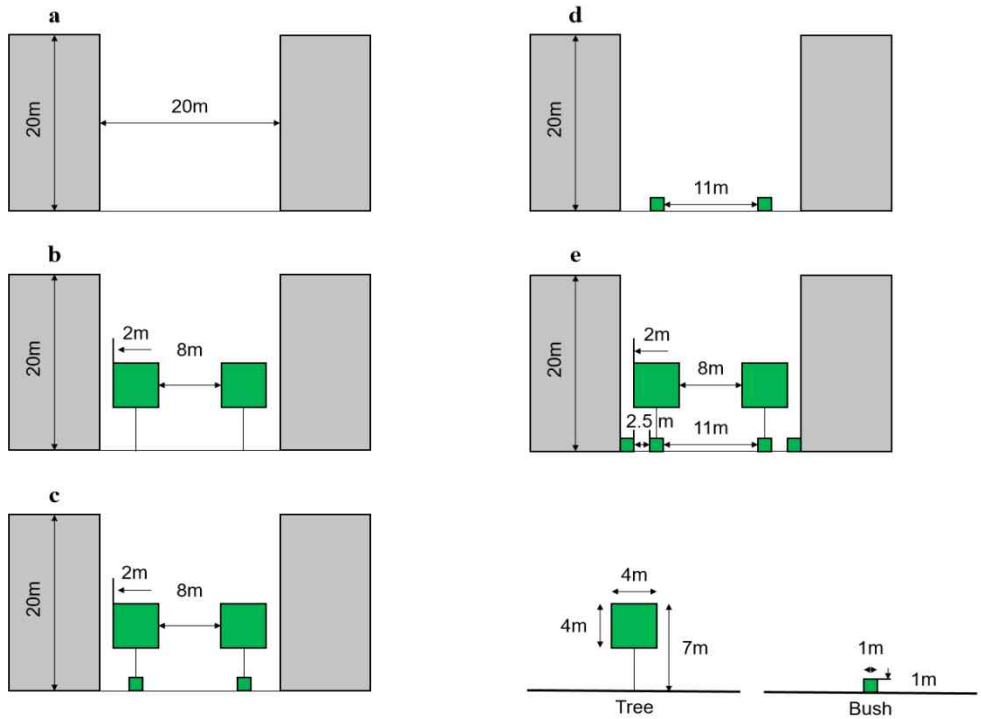

Figure 24. Intersection vegetation scenarios

Figures 2 and 3 show cross-shaped and T-shaped intersections, respectively. In this study, the five greening types illustrated in Figure 1 were applied to the street structures shown in Figures 2 and 3. Greening type a in Figure 1 corresponds to Cases A1 and B1 in Figures 2 and 3, b corresponds to Cases A2 and B2, c corresponds to Cases A3 and B3, d corresponds to Cases A4 and B4, and e corresponds to Cases A5 and B5. Figures 2 and 3 use different colors to indicate the locations of trees and

shrubs. The brown area in the middle represents the source of pollutants.

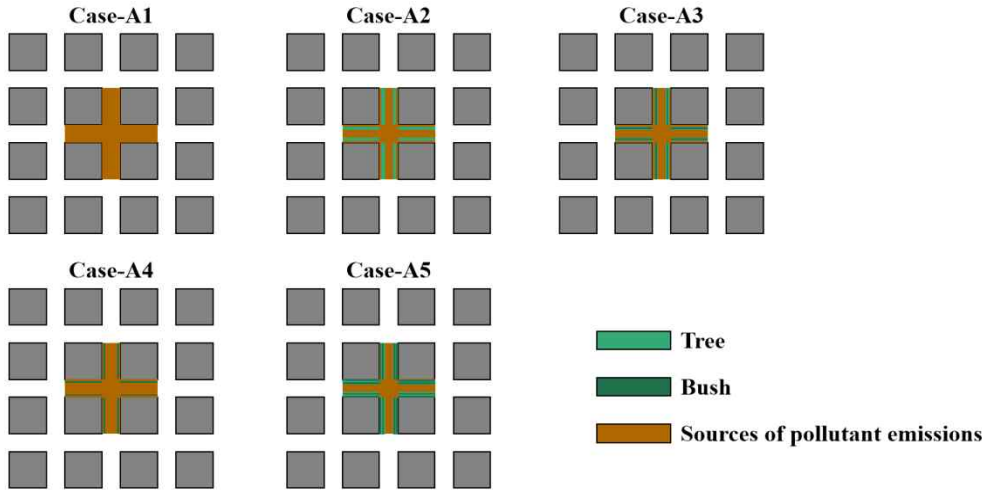

Figure 25. Cross-shaped intersection and the application of different greening types

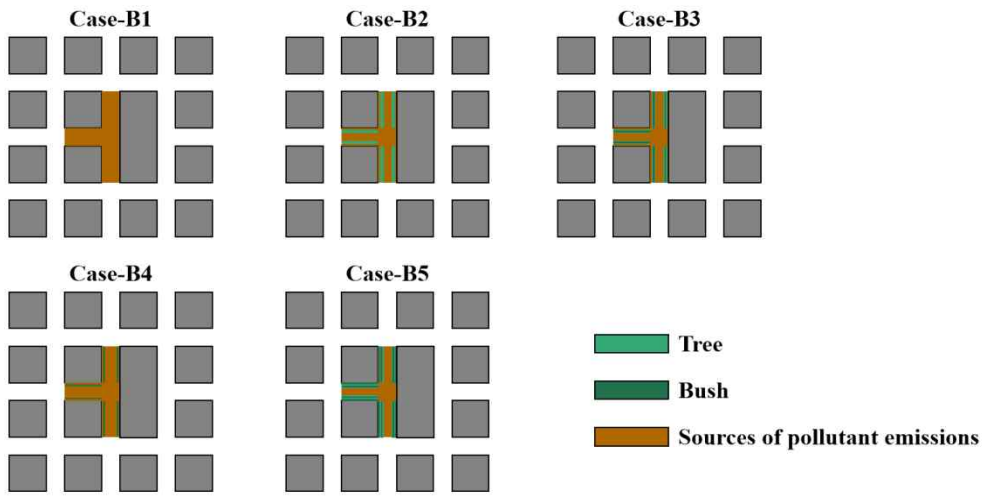

Figure 26. T-shaped intersection and the application of different greening types

The CFD scheme is a very effective method for simulation of the urban wind environment and urban pollutant diffusion. In this study, the calculation domain size was X = 1750 m, Y = 1750 m, Z = 1000 m, the

building height was set to X = 40 m, Y = 40 m, Z = 20 m, and the street width was set to 20 m. To calculate changes in wind speed and pollutant concentration accurately, the grid was refined around buildings, street canyons and vegetation. In this study, the central street in the model was set as the injection location of pollutant emissions. CO is a good tracer gas for simulation of pollutant diffusion in urban areas. In this study, CO was released uniformly at the bottom of the emission source area, and the emission source height was set to Z = 2 m (Guo X et al. 2021).

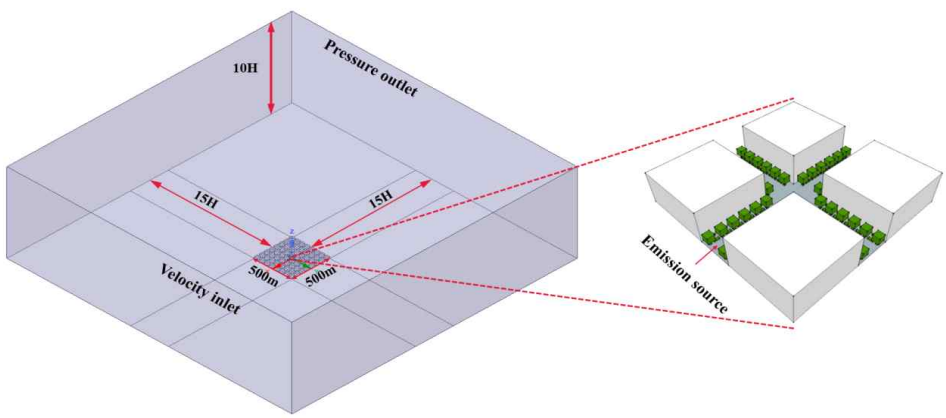

Figure 27. Calculation domain and pollutant emission source

3. Results

3.1. Influence of greening method on pollutants at a cross-shaped intersection

Figure 28 shows contour maps of wind speed and CO mass fraction at a cross-shaped intersection when the wind direction is westerly. First, due to the street canyon structure and wind direction, the wind speeds on the left and right sides of the X-axis are generally higher than in the upstream and downstream areas along the Y-axis. The maximum wind speed of case A1 is lower than the maximum wind speeds of cases A2, A3, A4, and A5. Trees provide the function of buffering wind speed and can be used as windbreak forests (Taleb H M et al. 2021). Average wind speed was highest in Case A1. Although trees and shrubs increase wind speed in a local area, leading to an increase in the maximum wind speed, vegetation reduces the overall average wind speed along the entire street. The lowest average wind speed appears in Case A5, as this case uses the greenest layout, resulting in a larger drop in average wind speed. In Cases A2, A3, and A5, the CO concentration increases near the buildings and vegetation on the leeward side of the Y-axis, where wind speed is lowest, as the wind cannot remove pollutants rapidly enough. However, in Cases A1 and A4, where only shrubs are used, the distribution of CO concentration is relatively uniform, with a tendency to increase on the right side of the X-axis and upstream portion of the Y-axis. In general, the area of high concentration tends to spread outward from the right side of the X-axis and upstream area of the Y-axis.

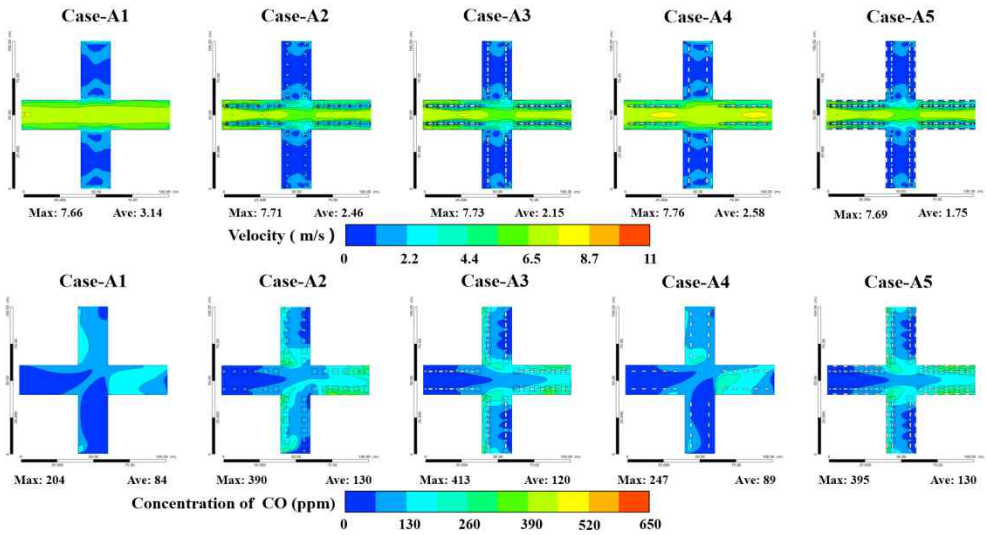

Figure 28. Contour maps of wind speed and CO concentration at a cross-shaped intersection

As shown in Figure 29, the maximum wind speeds in the street associated with the five greening methods show little difference, although the average wind speed changes markedly. The average wind speed in Case A1 without greenery is highest, and the second highest average wind speed appears in Case A4, which uses only shrubs for greening, while Cases A2, A3, and A5 include trees as a greening method. The average wind speed in the latter cases decreased more significantly than in the previous two cases. According to Table 1, when Case A1 without greenery is used as the standard, the average wind speed is greatly reduced with the application of greening methods. The average wind speed in Case A5 is reduced by 44.27%, while the average wind speed in Case A4 is reduced by 17.83%, and Cases A2 and A3 show reductions of

21.66% and 31.53%, respectively.

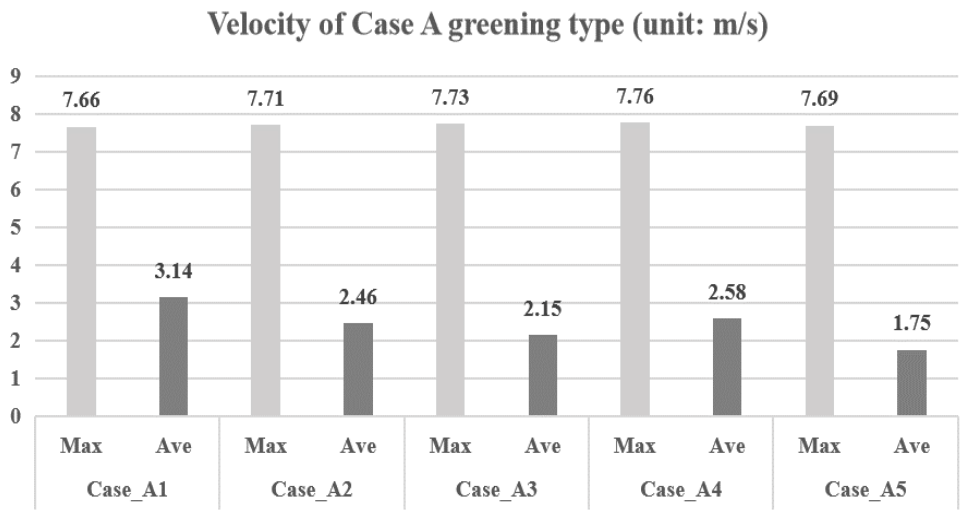

Figure 29. Wind speed changes at a cross-shaped intersection

As shown in Figure 30, the concentration of the pollutant CO exhibits a large range of changes in streets with different greening methods. The amplitude of the maximum concentration change is larger than the average concentration value. The cases with the largest maximum and average concentrations were Cases A2, A3, A5 using trees, while the smallest maximum and average concentrations were found in Case A1 without greening and Case A4 with shrubs only. Research into the effects of simple greening layouts (i.e., shrubs or trees located at four-way intersections) have shown that, in some cases, shrubs can enhance the diffusion of pollutants and increase ventilation, while trees increase the concentration of pollutants (Guo X et al. 2021). According to Table 1, Cases A2 and A5 produced the highest concentration increases relative to Case A1 without greening, at 54.76% for both cases, while the average

concentration increase for Case A3 was 42.86% and Case A4 had the smallest average increase in concentration, at 5.59%.

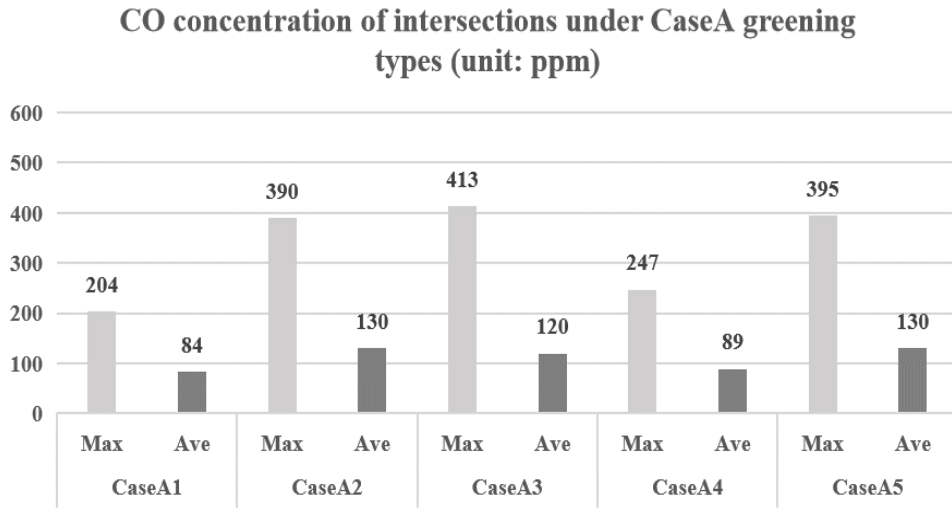

Figure 30. CO concentration changes at a cross-shaped intersection

Table 17. Wind speed and CO concentration change rates at a cross-shaped intersection

Greening type	Velocity			Concentration of CO		
	Average value	Variable value	Rate of change	Average value	Variable value	Rate of change
Case A1	3.14	x	x	84 ppm	x	x
Case A2	2.46	0.68	-21.66%	130 ppm	46 ppm	54.76%
Case A3	2.15	0.99	-31.53%	120 ppm	36 ppm	42.86%
Case A4	2.58	0.56	-17.83%	89 ppm	5 ppm	5.95%
Case A5	1.75	1.39	-44.27%	130 ppm	46 ppm	54.76%

3.2. Influence of greening method on pollutants at a T-shaped intersection

Figure 31 shows contour maps of a T-shaped intersection showing the wind speed and CO mass fraction when the wind is westerly. First, due to the street canyon structure and wind direction, wind speeds are generally lower on the upper and lower reaches of the Y-axis than along the X-axis. Wind enters from the left end of the X-axis and encounters building obstructions, causing it to spread along the upstream and downstream sides of the Y-axis; therefore, wind speeds on the leeward side of the upstream and downstream portions of the Y-axis are relatively low. The maximum wind speed in case B1 is lower than the maximum wind speeds in cases B2, B3, B4 and B5. Case B1 has the highest average wind speed. Although trees and shrubs increase wind speed in a local area, leading to an increase in the maximum wind speed, vegetation reduces the overall average wind speed along the entire street. The lowest average wind speed occurred in Case B5, which used the most greening. In Cases B2, B3, and B5, using trees for greening, the CO concentration increased near the buildings and vegetation on the leeward side of the Y-axis. In the T-shaped intersection structure, wind could not easily affect the upstream and downstream portions of the Y-axis. Therefore, the wind speed on the leeward side was relatively low, and the presence of vegetation sharpened the reduction in wind speed, resulting in a higher CO concentration in this area. In contrast, in the greening methods with only shrubs, Cases B1 and B4, CO diffuses quickly into wind at street level without being blocked by trees, resulting in a

relatively low CO concentration.

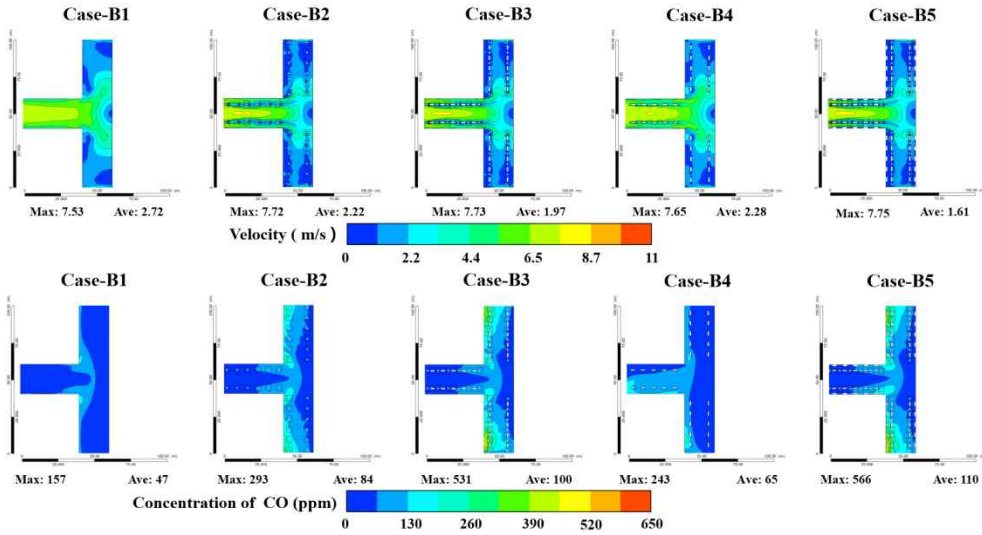

Figure 31. Contour maps of wind speed and pollutant concentration at a T-shaped intersection

According to Figure 32, the maximum wind speed at a T-shaped intersection shows small changes with all greening methods. The highest average wind speed occurs in Case B1 without greenery, the second highest average wind speed occurs in Case B4, which uses only shrubs for greening, and the lowest average wind speed is observed in Case B5. In general, greening methods without trees have higher average wind speeds than methods without trees. According to Table 2, when Case B1 is used as the standard, Case B5 has the greatest average wind speed reduction of 44.27%. The average wind speed in Case B3 is reduced by 31.53%, and the average wind speeds of Cases B2 and B4 are reduced by 21.66% and 17.83%, respectively.

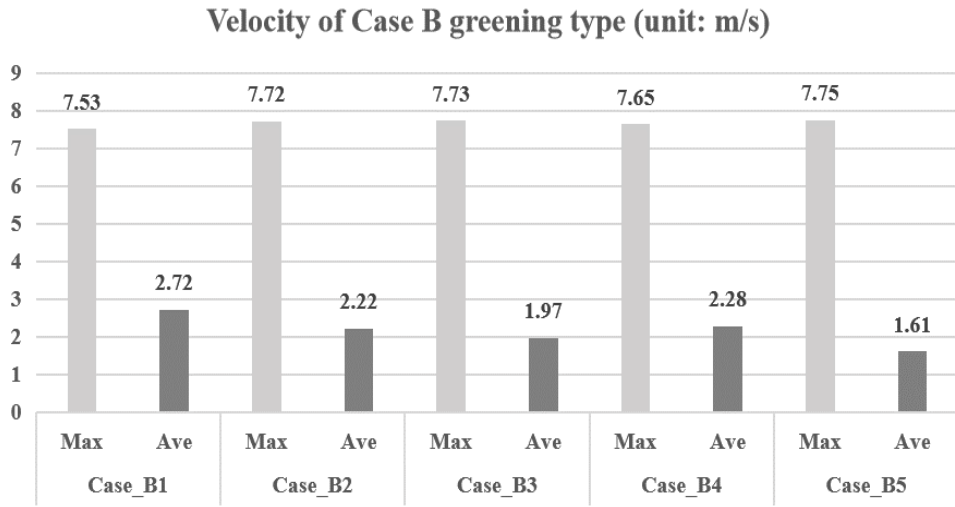

Figure 32. Wind speed changes at a T-shaped intersection

As shown in Figure 33, the concentration of the pollutant CO varies widely among streets with different greening methods. The maximum concentration is highest in Case B5, at 566 ppm, followed by Case B3, at 531 ppm. In contrast the lowest maximum value occurs in Case B1 without greenery, with a concentration of 157 ppm, followed by Case B4, which has only bushes and reaches 243 ppm. Table 2 indicates that when Case B1 without greenery is used as the standard, the average concentration increase rates in Cases B2, B3, B4, and B5 are 78.72%, 112.77%, 38.30%, and 134.04%, respectively. The largest increase in average concentration was in Case B5, which used the most greening methods, and the smallest increase was in Case B1, which had no greening.

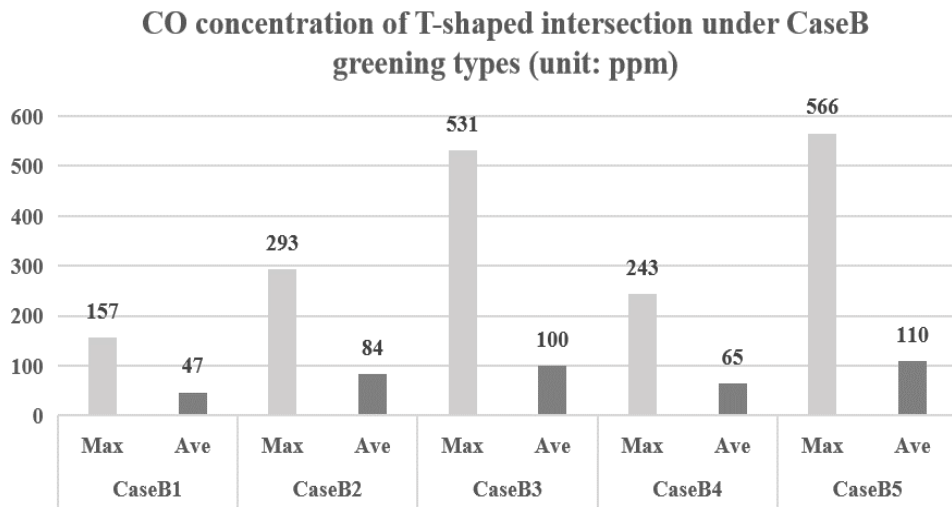

Figure 33. CO concentration changes at a T-shaped intersection

Table 18. Wind speed and CO concentration change rates at a T-shaped intersection

Greening type	Velocity			Concentration of CO		
	Average value	Variable value	Rate of change	Average value	Variable value	Rate of change
Case B1	2.72	x	x	47 ppm	x	x
Case B2	2.22	0.5	-18.38%	84 ppm	37 ppm	78.72%
Case B3	1.97	0.75	-27.57%	100 ppm	53 ppm	112.77%
Case B4	2.28	0.44	-16.18%	65 ppm	18 ppm	38.30%
Case B5	1.61	1.11	-40.81%	110 ppm	63 ppm	134.04%

4. Discussion

In chapter 4, CO was used as a representative pollutant, and then five greening patterns were applied to two intersection structures (cross-shaped and T-shaped) and the changes in average wind speed and CO concentration were observed. The results showed that, overall, when no greening was used as the standard, the average wind speed and CO concentration both increased the least when the greening method included only shrubs. According to the results presented in Tables 17 and 18, when only shrubs are used as the greening method, the average wind speed reduction at the cross-shaped intersection is 17.83%, and the increase in the average concentration of CO is also the smallest, at 5.95%. The average wind speed reduction at the T-shaped intersection is 16.18%, and the average CO concentration increase is 38.30%. In Cases A5 and B5, representing the greening methods with the most vegetation, the average wind speed reductions were the greatest, at 44.27% and 40.81%, respectively, and the average increase of the CO concentration reached its maximum values of 54.76% and 134.04%, respectively.

I propose that the diffusion of pollutants can be divided into two general cases, and the impact of greening on the concentration of pollutants may differ between these situations. First, wind mixed with pollutants may blow into an urban area under the premise that the atmospheric environment was previously clean. Second, urban areas may have high concentrations of pollutants, and clean wind may blow into those polluted areas. In the first case, reasonable greening methods may prevent the spread of pollutants in urban areas. Trees can be used as

natural windbreaks, and appropriate spacing between trees will reduce damage caused by the spread of pollutants in the city (Taleb et al. 2021). In the second case, greening may have the opposite effect. Vegetation in the city will reduce wind speed and reduce the diffusion rate of pollutants, and adsorption onto vegetation may also increase the concentration of pollutants in a local area.

Chapter 5 Conclusion

In this dissertation, three independent studies were conducted to simulate and analyze the large- and small-scale wind environment and pollutant diffusion in different situations, focusing on urban greening methods and relationships of building structures with the urban wind environment and pollutant diffusion.

Initially, in chapter 1, a study of the large-scale urban wind environment with and without greening showed that greening can provide the function of a windbreak forest in urban ventilation, reducing wind speed in urban areas, and that an appropriate greening layout can also guide wind direction. In a dense urban structure, little wind reaches the inner area of the city. Compared with a less dense urban structure, wind can more strongly affect the inner area, and greater changes in wind speed occurred in the inner area.

Chapter 2 focused on the effects of various greening methods and wind direction on wind speed in two structures, a small-scale built-up area and open area, and showed that wind direction has a strong influence on wind speed. When the study area is perpendicular to the wind direction, regardless of the urban structure, the average wind speed drops sharply. Meanwhile, regardless of wind direction, the combination of low-density two-row multilayer and high-density two-row multilayer plantings of trees and shrubs, which provided most vegetation among the greening methods tested, caused the largest decreases in wind speed. In the built-up area, the average wind speed showed an increasing trend,

while average wind speed decreased slightly in the open area.

Finally, in chapter 3, various greening methods were applied to cross-shaped and T-shaped intersections, and the impact of those greening methods on the diffusion of pollutants was simulated. Overall, with no greening as the standard, the use of only shrubs as a greening method led to the smallest increase in pollutant concentration, while the use of trees and shrubs together as a greening method led to the largest increase. When pollutant sources exist within the city, greening will have a negative effect, greatly reducing the rate of pollutant diffusion.

References

Amorim, J. H., Rodrigues, V., Tavares, R., Valente, J., & Borrego, C. (2013). CFD modelling of the aerodynamic effect of trees on urban air pollution dispersion. Science of the Total Environment, 461, 541-551.

Adamek, K., Vasan, N., Elshaer, A., English, E., & Bitsuamlak, G. (2017). Pedestrian level wind assessment through city development: A study of the financial district in Toronto. Sustainable cities and society, 35, 178-190.

Baetke, F., Werner, H., & Wengle, H. (1990). Numerical simulation of turbulent flow over surface-mounted obstacles with sharp edges and corners. Journal of wind engineering and industrial aerodynamics, 35, 129-147.

Blocken, B., Janssen, W. D., & van Hooff, T. (2012). CFD simulation for pedestrian wind comfort and wind safety in urban areas: General decision framework and case study for the Eindhoven University campus. Environmental Modelling & Software, 30, 15-34.

Blocken, B., & Carmeliet, J. (2004). Pedestrian wind environment around buildings: Literature review and practical examples. Journal of Thermal Envelope and Building Science, 28(2), 107-159.

Baik, J. J., Kang, Y. S., & Kim, J. J. (2007). Modeling reactive pollutant dispersion in an urban street canyon. Atmospheric Environment, 41(5), 934-949.

Cowan, I. R., Castro, I. P., & Robins, A. G. (1997). Numerical considerations for simulations of flow and dispersion around buildings.

Journal of Wind Engineering and Industrial Aerodynamics, 67, 535-545.

Di Sabatino, S., Buccolieri, R., Pulvirenti, B., & Britter, R. (2007). Simulations of pollutant dispersion within idealised urban-type geometries with CFD and integral models. Atmospheric environment, 41(37), 8316-8329.

Farr, D. (2011). Sustainable urbanism: Urban design with nature. John Wiley & Sons.

Guo, X., Gao, Z., Buccolieri, R., Zhang, M., & Shen, J. (2021). Effect of greening on pollutant dispersion and ventilation at urban street intersections. Building and Environment, 203, 108075.

Hang, J., Sandberg, M., Li, Y., & Claesson, L. (2010). Flow mechanisms and flow capacity in idealized long-street city models. Building and Environment, 45(4), 1042-1053.

Hang, J., Sandberg, M., & Li, Y. (2009). Effect of urban morphology on wind condition in idealized city models. Atmospheric Environment, 43(4), 869-878.

Hlavinka, M. W., & Bullin, J. A. (1988). Validation of mobile source emission estimates using mass balance techniques. Japca, 38(8), 1035-1039.

Jurado, X., Reiminger, N., Vazquez, J., & Wemmert, C. (2021). On the minimal wind directions required to assess mean annual air pollution concentration based on CFD results. Sustainable Cities and Society, 71, 102920.

Kwak, K. H., Baik, J. J., Ryu, Y. H., & Lee, S. H. (2015). Urban air quality simulation in a high-rise building area using a CFD model

coupled with mesoscale meteorological and chemistry-transport models. Atmospheric Environment, 100, 167-177.

Kang, G., Kim, J. J., & Choi, W. (2020). Computational fluid dynamics simulation of tree effects on pedestrian wind comfort in an urban area. Sustainable Cities and Society, 56, 102086.

Karim, A. A., & Nolan, P. F. (2011). Modelling reacting localized air pollution using Computational Fluid Dynamics (CFD). Atmospheric Environment, 45(4), 889-895.

Liu, C. H., Leung, D. Y., & Barth, M. C. (2005). On the prediction of air and pollutant exchange rates in street canyons of different aspect ratios using large-eddy simulation. Atmospheric Environment, 39(9), 1567-1574.

Murakami, S., & Mochida, A. (1989). Three-dimensional numerical simulation of turbulent flow around buildings using the k− ε turbulence model. Building and Environment, 24(1), 51-64.

Nishizawa, S., Sawachi, T., & Maruta, E. (2008). Evaluation of effect of the wind pressure fluctuation for cross ventilation in the residential district. In Proceedings of the Air Infiltration and Ventilation Centre Conference, Kyoto, Japan.

Pan, W., Qin, H., & Zhao, Y. (2017). Challenges for energy and carbon modeling of high-rise buildings: The case of public housing in Hong Kong. Resources, Conservation and Recycling, 123, 208-218.

Panagiotou, I., Neophytou, M. K. A., Hamlyn, D., & Britter, R. E. (2013). City breathability as quantified by the exchange velocity and its spatial variation in real inhomogeneous urban geometries: An example

from central London urban area. Science of the Total Environment, 442, 466-477.

Qin, H., Lin, P., Lau, S. S. Y., & Song, D. (2020). Influence of site and tower types on urban natural ventilation performance in high-rise high-density urban environment. Building and Environment, 179, 106960.

Soulhac, L., Perkins, R. J., & Salizzoni, P. (2008). Flow in a street canyon for any external wind direction. Boundary-Layer Meteorology, 126(3), 365-388.

Sanchez, B., Santiago, J. L., Martilli, A., Martin, F., Borge, R., Quaassdorff, C., & de la Paz, D. (2017). Modelling NOX concentrations through CFD-RANS in an urban hot-spot using high resolution traffic emissions and meteorology from a mesoscale model. Atmospheric Environment, 163, 155-165.

Taleb, H. M., & Kayed, M. (2021). Applying porous trees as a windbreak to lower desert dust concentration: Case study of an urban community in Dubai. Urban Forestry & Urban Greening, 57, 126915.

Tominaga, Y., & Stathopoulos, T. (2011). CFD modeling of pollution dispersion in a street canyon: Comparison between LES and RANS. Journal of Wind Engineering and Industrial Aerodynamics, 99(4), 340-348.

Wong, H. Y. (1979). A means of controlling bluff body flow separation. Journal of Wind Engineering and Industrial Aerodynamics, 4(2), 183-201.

Report

Seoul Institute(2020). [Climate change monitoring and simulation analysis by spatial type]

WHO(2014), 7 million premature deaths annually linked to air pollution

Nations, U. (2014). World urbanization prospects: The 2014 revision, highlights. department of economic and social affairs. Population Division, United Nations, 32.

World Health Organization. (2016). Ambient air pollution: A global assessment of exposure and burden of disease.

Website and others

ANSYS FLUENT 12.0 Theory Guide

Abstract (in Korean)

도시 형태에 따른 도시 바람환경 및 오염 물질 확산 CFD 분석

급격한 도시화는 도시지역의 건축물을 증가시키고, 도시지역의 풍속을 감소시키며, 대기순환에 영향을 미쳐 다양한 환경문제가 나타난다. 도시의 녹화는 도시의 바람 환경과 오염 물질 확산에 매우 중요한 역할이 있다. 많은 연구에서 녹화가 도시의 미기후, 바람 환경 및 오염 물질 확산에 미치는 영향을 무시하고 건물의 구조와 밀도에만 집중한다. 이 논문에서는 CFD 모델을 사용하여 다양한 도시 구조와 존재 여부의 영향을 시뮬레이션하였다. 첫째, 도시 환기에 대한 녹화. 둘째, 수평 및 수직 바람의 영향을 시뮬레이션하기 위해 다양한 공간 유형과 녹화 유형을 사용했다. 셋째, 여러 녹지 유형이 서로 다른 구조의 도시 교차로에서 오염 물질 확산에 미치는 영향을 시뮬레이션했다. 3개의 독립적인 연구에서 도시 녹화, 건물 구조 및 오염 물질 확산 간의 관계를 탐구하는 데 중점을 두었다.

연구지역은 저층 주거지역 제기동 주민센터, 고층 상업지역 강남구청을 선정하였다. 전통 방법 중 모니터링 스테이션 데이터와 측정 장비로 현장 조사. 그러나 이러한 방법은 소규모 도시 공간에서 상대적으로 시간과 비용이 많이 소요되고 정확도가 상대적으로 낮다. 이러한 한계를 극복하기 위해 상용 CFD(전산 유체 역학) 모델은 바람 환경, 오염 물질 분산 및 도시 열섬 효과와 같은 미기후 효과를 시뮬레이션하는 데 중요한 도구가 되고 있다. CFD 모델의 주요 장점은 도시 모델을 현실에 가까운 상태로 축

소할 수 있다는 것이다. 또한 도시 지역에 대한 건물 정보와 CFD 소프트웨어를 결합하여 바람의 흐름뿐만 아니라 도시의 오염 물질 확산 경로를 평가하여 고효율로 신속한 시뮬레이션이 가능하다.

녹화가 있거나 없는 대규모 도시 바람 환경에 대한 연구에 따르면 녹화는 도시 환기에서 방풍림의 기능을 제공하고 도시 지역의 풍속을 감소시키며 적절한 녹화 방안도 안내할 수 있음을 보여준다. 고밀한 도시구조에서 바람은 도시의 내부에 거의 도달하지 않으며. 저밀한 도시구조에서 바람은 내부 지역에 더 강하게 영향을 미칠 수 있으며 내부 지역에서 풍속의 변화가 더 크다.

연구지역이 풍향에 수직일 경우 도시구조의 영향 없이 평균 풍속은 급격히 떨어진다. 한편, 풍향에 영향 없이 테스트한 녹화 방법중 저밀도 2열 다층식재와 고밀도 2열 다층식재의 조합이 가장 큰 풍속 저감을 일으켰다. 시가지에서는 평균 풍속이 증가하는 경향을 보인 반면, 개방된 지역에서는 평균 풍속이 감소 하였다. 전체적으로 녹화가 없는 것을 기준으로 관목만을 사용했을 때 가장 적은 풍속증가가 보였다. 오염 물질 농도는 수목과 관목을 함께 녹화하는 방식이 농도가 제일 크게 증가 했다. 오염원이 도시 내에 존재하면 녹화는 부정적인 영향을 미치고 오염 물질 확산 속도를 크게 감소할수 있다.

따라서 본 연구에서는 CFD 모델을 사용하여 도시 미기후를 시뮬레이션하는 방법을 설명하고 이 방법을 도시 계획에 실시간으로 적용하여 이전 방법의 평균보다 높은 정확도를 제공하는 것을 목표로 한다.

주요어 : 전산유체역학, 미기후, 오염물질 확산, 도시형 교차로, 거리녹화

학번: 2019-24202